Please cite this article in press as: Riemer et al., ITPK1 is an $InsP_6$/ADP phosphotransferase that controls phosphate signaling in *Arabidopsis*, Molecular Plant (2021), https://doi.org/10.1016/j.molp.2021.07.011

Molecular Plant
Research article

CellPress
Partner Journal

ITPK1 is an $InsP_6$/ADP phosphotransferase that controls phosphate signaling in *Arabidopsis*

Esther Riemer[1,9], Danye Qiu[2,9], Debabrata Laha[3,4], Robert K. Harmel[5,6], Philipp Gaugler[1], Verena Gaugler[1], Michael Frei[7], Mohammad-Reza Hajirezaei[8], Nargis Parvin Laha[1], Lukas Krusenbaum[1], Robin Schneider[1], Adolfo Saiardi[3], Dorothea Fiedler[5,6], Henning J. Jessen[2], Gabriel Schaaf[1,*] and Ricardo F.H. Giehl[8,*]

[1]Department of Plant Nutrition, Institute of Crop Science and Resource Conservation, Rheinische Friedrich-Wilhelms-Universität Bonn, 53115 Bonn, Germany

[2]Department of Chemistry and Pharmacy and CIBSS-Centre for Integrative Biological Signalling Studies, Albert-Ludwigs University Freiburg, 79104 Freiburg, Germany

[3]Medical Research Council Laboratory for Molecular Cell Biology (MRC-LMCB), University College London, London WC1E 6BT, UK

[4]Department of Biochemistry, Indian Institute of Science, Bengaluru, Karnataka 560 012, India

[5]Leibniz-Forschungsinstitut für Molekulare Pharmakologie, 13125 Berlin, Germany

[6]Department of Chemistry, Humboldt Universität zu Berlin, 12489 Berlin, Germany

[7]Institute of Agronomy and Crop Physiology, Justus-Liebig University Giessen, 35392 Giessen, Germany

[8]Department of Physiology & Cell Biology, Leibniz-Institute of Plant Genetics and Crop Plant Research, 06466 Gatersleben, Germany

[9]These authors contributed equally to this article

***Correspondence: Gabriel Schaaf (gabriel.schaaf@uni-bonn.de), Ricardo F.H. Giehl (giehl@ipk-gatersleben.de)**

https://doi.org/10.1016/j.molp.2021.07.011

ABSTRACT

In plants, phosphate (P_i) homeostasis is regulated by the interaction of PHR transcription factors with stand-alone SPX proteins, which act as sensors for inositol pyrophosphates. In this study, we combined different methods to obtain a comprehensive picture of how inositol (pyro)phosphate metabolism is regulated by P_i and dependent on the inositol phosphate kinase ITPK1. We found that inositol pyrophosphates are more responsive to P_i than lower inositol phosphates, a response conserved across kingdoms. Using the capillary electrophoresis electrospray ionization mass spectrometry (CE-ESI-MS) we could separate different $InsP_7$ isomers in *Arabidopsis* and rice, and identify 4/6-$InsP_7$ and a PP-$InsP_4$ isomer hitherto not reported in plants. We found that the inositol pyrophosphates 1/3-$InsP_7$, 5-$InsP_7$, and $InsP_8$ increase several fold in shoots after P_i resupply and that tissue-specific accumulation of inositol pyrophosphates relies on ITPK1 activities and MRP5-dependent $InsP_6$ compartmentalization. Notably, ITPK1 is critical for P_i-dependent 5-$InsP_7$ and $InsP_8$ synthesis *in planta* and its activity regulates P_i starvation responses in a PHR-dependent manner. Furthermore, we demonstrated that ITPK1-mediated conversion of $InsP_6$ to 5-$InsP_7$ requires high ATP concentrations and that *Arabidopsis* ITPK1 has an ADP phosphotransferase activity to dephosphorylate specifically 5-$InsP_7$ under low ATP. Collectively, our study provides new insights into P_i-dependent changes in nutritional and energetic states with the synthesis of regulatory inositol pyrophosphates.

Key words: inositol phosphates, inositol pyrophosphates, phosphate homeostasis, phosphate signaling, inositol 1,3,4-trisphosphate 5/6-kinase 1, diphosphoinositol pentakisphosphate kinase

Riemer E., Qiu D., Laha D., Harmel R.K., Gaugler P., Gaugler V., Frei M., Hajirezaei M.-R., Laha N.P., Krusenbaum L., Schneider R., Saiardi A., Fiedler D., Jessen H.J., Schaaf G., and Giehl R.F.H. (2021). ITPK1 is an $InsP_6$/ADP phosphotransferase that controls phosphate signaling in *Arabidopsis*. Mol. Plant. **14**, 1–17.

INTRODUCTION

To maintain cellular phosphate (P_i) homeostasis, plants have evolved complex sensing and signaling mechanisms that adjust whole-plant P_i demand with external P_i availability. Although

Published by the Molecular Plant Shanghai Editorial Office in association with Cell Press, an imprint of Elsevier Inc., on behalf of CSPB and CEMPS, CAS.

Please cite this article in press as: Riemer et al., ITPK1 is an $InsP_6$/ADP phosphotransferase that controls phosphate signaling in *Arabidopsis*, Molecular Plant (2021), https://doi.org/10.1016/j.molp.2021.07.011

many molecular players involved in these responses have been identified, the exact mechanism of P_i sensing in complex organisms, such as plants, still remains largely unknown. In the model species *Arabidopsis thaliana*, the MYB transcription factors PHOSPHATE STARVATION RESPONSE 1 (PHR1) and its closest paralog PHR1-LIKE1 (PHL1) control the expression of the majority of P_i starvation-induced (PSI) genes to regulate numerous metabolic and developmental adaptations induced by P_i deficiency (Rubio et al., 2001; Bustos et al., 2010). Since *PHR1* expression is only weakly responsive to P_i deficiency (Rubio et al., 2001), the existence of a post-translational control of PHR1 and PHL1 factors has been proposed. Emerging evidence indicates that a class of stand-alone SPX proteins negatively regulates the activity of PHR transcription factors in different plant species (Liu et al., 2010; Wang et al., 2014b; Lv et al., 2014; Puga et al., 2014; Qi et al., 2017; Zhong et al., 2018; Ried et al., 2021). In *Arabidopsis*, SPX proteins can interact with the plant-unique coiled-coil motif of PHR1, thereby controlling the oligomeric state and the promoter binding activity of this transcription factor (Ried et al., 2021).

The *in vivo* interaction of PHRs and SPXs is influenced by P_i (Wang et al., 2014b; Lv et al., 2014; Puga et al., 2014), suggesting that this mechanism could represent a direct link between P_i perception and downstream signaling events. However, the dissociation constants for P_i itself in an SPX–PHR complex ranged from 10 mM to 20 mM (Wang et al., 2014b; Lv et al., 2014; Puga et al., 2014). The study of Wild et al. (2016) demonstrated that SPX domains act as receptors for inositol pyrophosphates (PP-InsPs), small signaling molecules consisting of a phosphorylated *myo*-inositol ring and one or two pyrophosphate groups (Wilson et al., 2013; Shears, 2018). Isothermal titration calorimetry experiments demonstrated that 5PP-$InsP_5$ (hereafter 5-$InsP_7$) interacts more strongly with SPX domains than P_i (Wild et al., 2016). More recent studies have further shown that 1,5(PP)$_2$-$InsP_4$ (1,5-$InsP_8$ hereafter) has an even higher binding affinity toward SPX domains than 5-$InsP_7$ *in vitro* (Gerasimaite et al., 2017; Dong et al., 2019; Ried et al., 2021), and that $InsP_8$ can restore more efficiently the interaction between SPX1 and PHR1 *in vivo* (Dong et al., 2019). In line with the proposed role of $InsP_8$ as an intracellular P_i signaling molecule controlling the formation of SPX–PHR complexes, *Arabidopsis* mutants with compromised synthesis of PP-InsPs exhibit constitutive PSI gene expression and overaccumulate P_i (Stevenson-Paulik et al., 2005; Kuo et al., 2014, 2018; Dong et al., 2019; Zhu et al., 2019). Importantly, cellular pools of different PP-InsPs are significantly altered in response to P_i availability in *Arabidopsis* (Kuo et al., 2018; Dong et al., 2019), suggesting that the enzymes involved in their synthesis could act as regulators of P_i homeostasis in plants. However, the biosynthetic steps leading to dynamic changes in $InsP_8$ levels in response to P_i availability still remain unresolved.

In plants, synthesis of $InsP_8$ is mediated by VIH1 and VIH2 (Laha et al., 2015; Dong et al., 2019; Zhu et al., 2019), a class of bifunctional kinase/phosphatase enzymes (Zhu et al., 2019) sharing homology with the yeast and animal Vip1/PPIP5Ks (Desai et al., 2014; Laha et al., 2015). However, how plants synthesize $InsP_7$ has since long remained elusive, as plant genomes do not encode homologs of the metazoan and yeast $InsP_6$ kinases IP6K/Kcs1 (Saiardi et al., 1999). We and others have recently identified the *Arabidopsis* inositol 1,3,4-trisphosphate 5/6-kinases ITPK1 and ITPK2 as putative novel plant $InsP_6$ kinases (Adepoju et al., 2019; Laha et al., 2019). We further showed that ITPK1 generates the meso $InsP_7$ isomer 5-$InsP_7$, the major form identified in seed extracts (Laha et al., 2019). Furthermore, $InsP_7$ and $InsP_8$ levels are compromised in an itpk1 mutant, showing that ITPK1 functions as an $InsP_6$ kinase *in planta* (Laha et al., 2019). Since $InsP_7$ is the precursor for $InsP_8$ synthesis, the next challenge is to determine which $InsP_7$ isomers respond to P_i and how their synthesis is linked to the plant's P_i status. A recent study reported that P_i deficiency induces a shoot-specific increase in $InsP_7$ levels in *Arabidopsis* as determined by high-performance liquid chromatography (HPLC) analysis of [^{32}P]P_i-labeled extracts (Kuo et al., 2018). However, this response does not easily explain decreased $InsP_8$ levels detected in shoots of P_i-deficient *Arabidopsis* plants by polyacrylamide gel electrophoresis (PAGE) (Dong et al., 2019). Since ^{32}P labeling does not provide a mass assay of the inositol species, and PAGE is not suited to the analysis of lower inositol phosphates (InsPs), alternative approaches are still required to obtain a complete picture of P_i-dependent metabolism of InsPs and PP-InsPs in plants. The recent development of a capillary electrophoresis electrospray ionization mass spectrometry (CE-ESI-MS) method for ultrasensitive analysis of inositol (pyro)phosphates (Qiu et al., 2020) offers a unique opportunity to perform isomer identification and quantitation in different plant tissues.

Here, we combined [^{3}H]inositol labeling, PAGE, and CE-ESI-MS to investigate in unprecedented detail P_i-, ITPK1-, and VIH2-dependent quantitative changes in inositol (pyro)phosphate levels. Our results reveal sensitive responses of 1/3-$InsP_7$, 5-$InsP_7$, and $InsP_8$ according to cellular P_i levels and organ-specific accumulation of $InsP_7$ and $InsP_8$ relying on MRP5-dependent $InsP_6$ compartmentalization. We also identified two previously unreported PP-InsP isomers, including a presumptive PP-$InsP_4$ isomer that is preferentially produced in roots in an ITPK1-dependent manner. With grafting and genetic crosses, we demonstrate that ITPK1 activity in shoots is more critical for undisturbed P_i signaling and relies on functional PHRs. Finally, we show that *Arabidopsis* ITPK1 mediates adenylate charge-dependent reversible reactions with high K_M values for ATP and ADP, and generates 5-$InsP_7$ *in planta*, which we determined to be the main substrate for the strong $InsP_8$ synthesis induced by P_i resupply to P_i-starved plants.

RESULTS

P_i-dependent synthesis of PP-InsPs is conserved across multicellular organisms

To assess if the synthesis of $InsP_8$ and its immediate precursor, $InsP_7$, responds to quick changes in P_i availability, we analyzed $InsP_6$, $InsP_7$, and $InsP_8$ levels with the help of titanium dioxide (TiO_2)-based pull-down followed by separation via PAGE (Losito et al., 2009; Wilson et al., 2015). In the dicotyledonous species *A. thaliana*, total phosphorus (P) concentration in shoots decreased significantly after 7 days of growth in a P_i-deficient nutrient solution (Figure 1A). When P_i was resupplied, shoot P levels were already significantly increased after 6 h and reached levels comparable to those of plants cultivated continuously on P_i-replete conditions after 12 h. In

Please cite this article in press as: Riemer et al., ITPK1 is an $InsP_6$/ADP phosphotransferase that controls phosphate signaling in *Arabidopsis*, Molecular Plant (2021), https://doi.org/10.1016/j.molp.2021.07.011

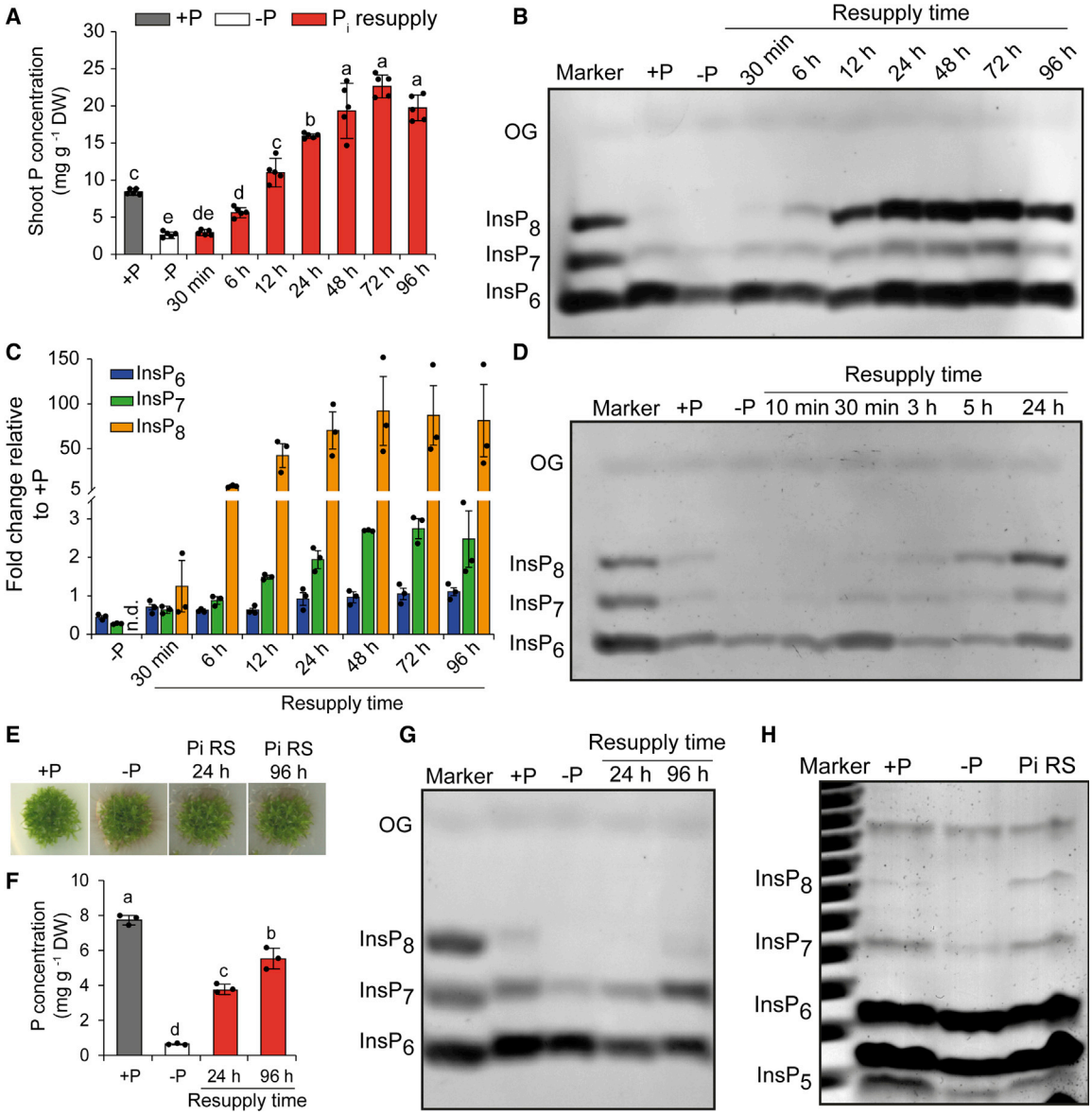

Figure 1. P_i-dependent regulation of $InsP_7$ and $InsP_8$ levels is conserved in multicellular organisms.

(A) Shoot total P levels in *A. thaliana* in response to sufficient (+P) or deficient P_i (−P) or after P_i resupply to P_i-starved plants for the indicated time. Data are means ± SD (n = 5 plants).

(B and C) Time-course PAGE analysis of inositol (pyro)phosphates in response to P_i starvation and P_i resupply in *A. thaliana* shoots **(B)** and fold change of quantified signal intensities **(C)**. Data are means ± SE (n = 3 gels loaded with independent biological samples). n.d., not detected. OG, orange G.

(D) Time-course PAGE analysis of rice shoots. Plants were cultivated in hydroponics under sufficient P_i (+P) or deficient P_i (−P) for 7 days (*A. thaliana* Col-0) or 10 days (rice, *Oryza sativa* cv. Nipponbare), or –P resupplied with P_i for the indicated times. Quantification of signals is shown in Supplemental Figure 1. OG, orange G.

(E–G) Phenotype **(E)**, total P_i levels **(F)**, and PAGE analysis **(G)** of gametophores of *Physcomitrium patens*. Plants were cultivated on sufficient P_i (+P), starved of P_i for 30 days (−P), or resupplied with P_i for the indicated time. Data are means ± SD (n = 3 biological replicates). OG, orange G.

(H) PAGE analysis of inositol (pyro)phosphates extracted from HCT116 cells cultured on sufficient P_i (+P), starved in P_i-free medium for 18 h (−P), or −P and resupplied with P_i for 3.5 h (Pi RS). Cells were harvested at the same time. The experiment was repeated twice with similar results.

In **(A)** and **(F)**, different letters indicate significant differences according to Tukey's test ($P < 0.05$).

the same plants, $InsP_6$, $InsP_7$, and $InsP_8$ signals decreased significantly in response to P_i starvation (Figure 1B and 1C). However, the most dramatic changes were observed when P_i-starved plants were resupplied with P_i. In relative terms, $InsP_7$ and $InsP_8$ responded much more sensitively to P_i resupply than $InsP_6$, with $InsP_8$ signals increasing almost 100-fold and greatly surpassing the levels detected in plants grown constantly under sufficient P_i (Figure 1C). Strong recovery of $InsP_7$ and especially $InsP_8$ was also detected in shoots of the monocotyledonous species rice (Figure 1D and Supplemental Figure 1). We could also detect clear P_i-dependent accumulation of PP-InsPs in gametophores of the moss

Please cite this article in press as: Riemer et al., ITPK1 is an $InsP_6$/ADP phosphotransferase that controls phosphate signaling in *Arabidopsis*, Molecular Plant (2021), https://doi.org/10.1016/j.molp.2021.07.011

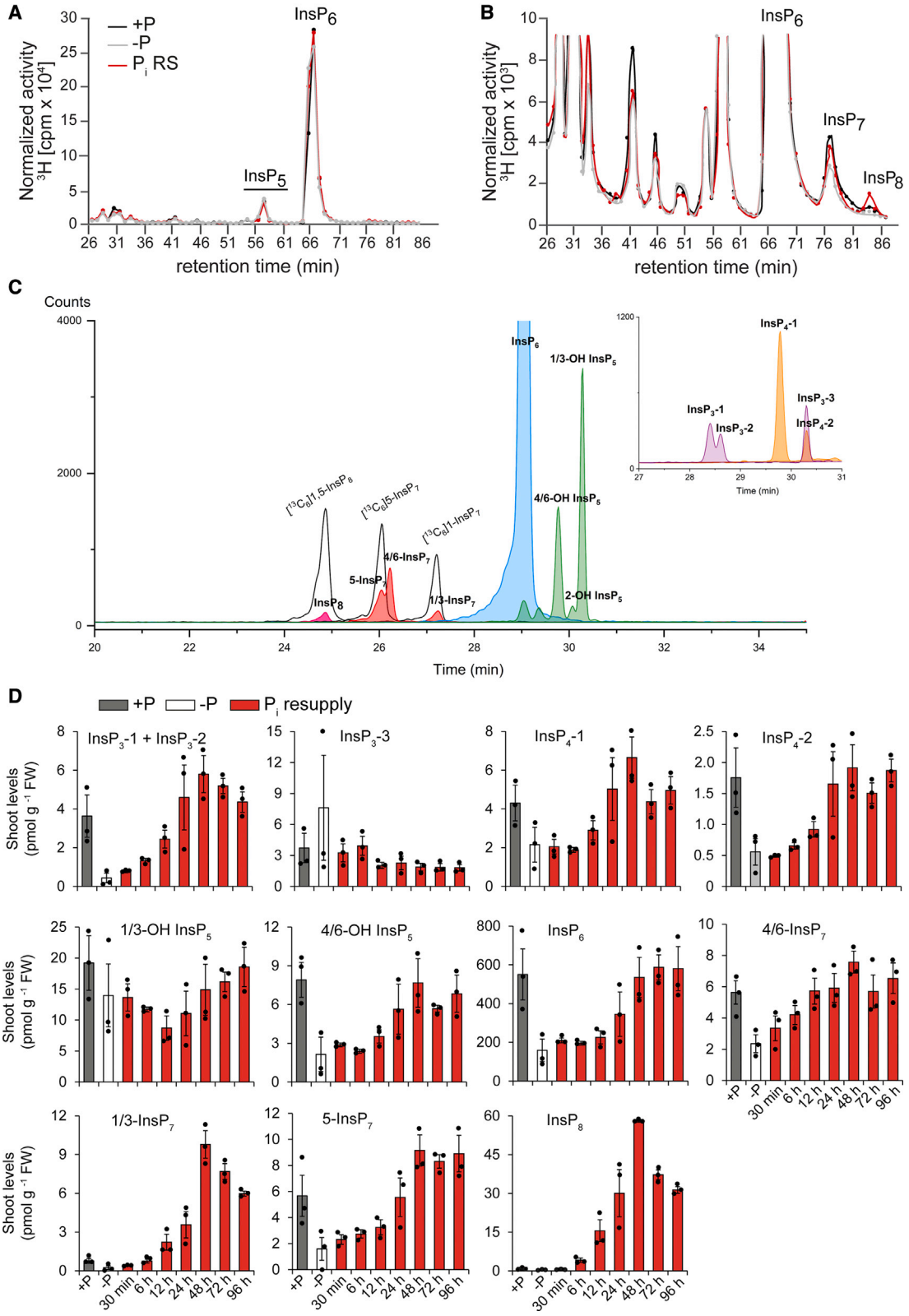

Figure 2. InsP and PP-InsP profiles in response to changes in P_i availability.

(A and B) HPLC profiles of *Arabidopsis* (Col-0) seedlings radiolabeled with [^{3}H]*myo*-inositol. Seedlings were grown with P_i (+P) or without P_i (−P) or −P resupplied with P_i for 6 h (P_i RS). Full, normalized spectra **(A)** and zoom-in view of the same profile **(B)**. The experiment was repeated with similar results, and representative results from one experiment are shown.

(legend continued on next page)

Please cite this article in press as: Riemer et al., ITPK1 is an $InsP_6$/ADP phosphotransferase that controls phosphate signaling in *Arabidopsis*, Molecular Plant (2021), https://doi.org/10.1016/j.molp.2021.07.011

Physcomitrium patens, although induction by P_i resupply was less pronounced in this species (Figure 1E–1G). Together, these results suggest that P_i-dependent $InsP_7$ and $InsP_8$ synthesis is conserved in vascular and non-vascular land plants. We also used PAGE to assess P_i-dependent synthesis of PP-InsPs in the human HCT116 cell line, and found that while $InsP_6$ levels remained largely unaffected by P_i conditions, both $InsP_7$ and $InsP_8$ decreased in cells after P_i was removed from the culture and sharply increased again after P_i resupply (Figure 1H). Altogether, these results indicate that P_i-dependent synthesis of $InsP_7$ and $InsP_8$ seems to be evolutionarily conserved across a range of multicellular organisms.

Comprehensive analysis of P_i-dependent inositol (pyro) phosphate metabolism in *Arabidopsis*

As PAGE separation and staining cannot detect lower InsPs and is unable to distinguish PP-InsP regioisomers (Losito et al., 2009), we used additional methods to investigate in more detail which InsPs and PP-InsPs respond to P_i. First, we performed strong anion-exchange chromatography–HPLC analyses of extracts from [^{3}H]inositol-labeled wild-type (WT) seedlings. Of all InsPs detected in whole seedlings, only $InsP_6$ and the PP-InsPs $InsP_7$ and $InsP_8$ decreased in response to P_i starvation and increased again after P_i resupply (Figure 2A and 2B). Two $InsP_4$ isomers of unknown isomeric nature (eluting at 41 and 46 min, respectively) also decreased under P_i deficiency, but none of the lower InsPs exhibited a comparable fast recovery after P_i resupply relative to $InsP_7$ and $InsP_8$ (Figure 2A and 2B).

Next, we used the recently developed CE-ESI-MS method, which does not rely on metabolic labeling and is therefore not blind to inositol derivatives generated *de novo* from D-glucose-6-phosphate (Qiu et al., 2020). To validate the method with plant samples of 6-week-old plants grown in hydroponics, assignment of 1-$InsP_7$, 5-$InsP_7$, and 1,5-$InsP_8$ was confirmed with fully ^{13}C-labeled internal standards (Figure 2C). Except for $InsP_3$-3 and 1/3-OH $InsP_5$, the remaining InsPs and all PP-InsPs detected with CE-ESI-MS decreased in P_i-deficient shoots (Figure 2D). Within a maximum of 12 h of P_i resupply, PP-InsP levels had recovered to P_i-sufficient levels, while at least 24 h was required to restore the levels of InsPs. In line with our PAGE analysis, $InsP_8$ showed the most dramatic relative change (up to a 40-fold increase), with levels surpassing those detected in P_i-sufficient plants already after 6 h of P_i resupply (Figure 2D). 1/3-$InsP_7$ also experienced a fast recovery during P_i resupply. We found that 5-$InsP_7$ was more abundant than 1/3-$InsP_7$ and also responded to P_i resupply, although less sensitively than 1/3-$InsP_7$ and $InsP_8$ (Figure 2D). Remarkably, we also detected a previously unreported $InsP_7$ isomer that migrated separately from [$^{13}C_6$]5-$InsP_7$ and [$^{13}C_6$]1-$InsP_7$ standards and co-migrated with synthetic 6-$InsP_7$ (Capolicchio et al., 2013), hence likely representing 4-$InsP_7$ or the 6-$InsP_7$ enantiomer (Supplemental Figure 2). Unlike 1/3-$InsP_7$ and 5-$InsP_7$, the novel $InsP_7$ isomer responded only mildly to P_i starvation and P_i resupply (Figure 2D). Together, these results demonstrate that, although most InsPs and PP-InsPs decrease during P_i deficiency, the levels of the PP-InsPs 1/3-$InsP_7$, 5-$InsP_7$, and $InsP_8$ recover faster and more strongly compared with all other InsP species when P_i-starved plants regain access to P_i.

The synthesis of 1/3-$InsP_7$, 5-$InsP_7$, and $InsP_8$ is tightly linked to cellular P_i levels

The widespread effects of P_i starvation and P_i resupply on most InsPs and PP-InsPs are not unexpected, as the synthesis of these molecules relies on available P_i for the phosphorylation reactions. However, the most sensitive response of 1/3-$InsP_7$, 5-$InsP_7$, and $InsP_8$ to P_i refeeding suggested that their synthesis might be more directly associated with a signaling mechanism. To test this hypothesis, we compared P_i-supplied WT plants and the P-overaccumulating mutant *pho2-1* (Delhaize and Randall, 1995), defective in the E2 ubiquitin conjugase-related enzyme PHO2 (also known as UBC24) (Aung et al., 2006; Bari et al., 2006; Lin et al., 2008). Under our growth conditions, *pho2-1* plants overaccumulated P in shoots as expected (Figure 3A). PAGE revealed that $InsP_7$ and especially $InsP_8$ signals were significantly increased in *pho2-1*, while $InsP_6$ was hardly affected (Figure 3B). Subsequent CE-ESI-MS analysis showed that none of the detected lower InsP isomers was significantly increased in shoots of *pho2-1* plants (Figure 3C). In contrast, $InsP_8$ was increased approximately 50-fold in *pho2* shoots, further reinforcing that $InsP_8$ is the most P_i-sensitive PP-InsP in leaves. Whereas the levels of the novel presumptive 4/6-$InsP_7$ isomer did not change considerably in *pho2-1*, 5-$InsP_7$ exhibited a clear increase, albeit less dramatic than that of 1/3-$InsP_7$ (Figure 3C). Altogether, these results demonstrate that the synthesis of 1/3-$InsP_7$, 5-$InsP_7$, and $InsP_8$ is tightly controlled by a mechanism that relays changes in cellular P_i levels specifically toward PP-InsP biosynthesis.

ITPK1 is required for P_i-dependent synthesis of 1/3-$InsP_7$, 5-$InsP_7$, and $InsP_8$ *in planta*

Previously, the analysis of [^{32}P]P_i-labeled seedlings indicated that *itpk1* mutant plants display decreased levels of $InsP_6$ and $InsP_7$ and increased levels of InsP(3,4,5,6)P_4 and its enantiomer (Kuo et al., 2018). Analysis of [^{3}H]inositol-labeled seedlings showed that not only $InsP_7$ but also $InsP_8$ levels are decreased in the *itpk1* mutant (Laha et al., 2020). However, the function of ITPK1 in P_i-dependent synthesis of specific $InsP_7$ isomers and its link to VIH1/VIH2 remain unclear. Under our growth conditions, *itpk1* plants overaccumulated P whenever P_i was supplied in the nutrient solution, while *vih2-4* accumulated significantly more P than WT only during short P_i resupply (Figure 4A). P_i-resupply-induced $InsP_8$ accumulation was compromised in *itpk1* and *vih2-4* single mutants, whereas $InsP_7$ levels were decreased in *itpk1* irrespective of the P_i regime (Figure 4B). Importantly, the defective synthesis of $InsP_7$ and $InsP_8$ of *itpk1* could be largely

(C) Extracted-ion electropherograms of InsPs and PP-InsPs in *Arabidopsis* (Col-0) shoots. $InsP_8$, 5-$InsP_7$, and 1/3-$InsP_7$ were assigned by mass spectrometry and identical migration time compared with their heavy isotopic standards. A new PP-InsP isomer was assigned as 4/6-$InsP_7$, based on proofs showed in Supplemental Figure 2. Assignment of $InsP_6$ and $InsP_5$ is according to mass spectrometry and identical migration time compared with relative standards. Inset shows extracted-ion electropherograms of three $InsP_3$ and two $InsP_4$ isomers.
(D) CE-ESI-MS analysis of inositol (pyro)phosphate levels in shoots of *Arabidopsis* (Col-0) plants exposed to variable P_i supplies. Plants were cultivated in hydroponics under sufficient P_i (+P), deficient P_i for 7 days (−P), or −P resupplied with P_i for the indicated times. Data are means ± SE (n = 3 biological replicates composed of two plants each).

Please cite this article in press as: Riemer et al., ITPK1 is an $InsP_6$/ADP phosphotransferase that controls phosphate signaling in *Arabidopsis*, Molecular Plant (2021), https://doi.org/10.1016/j.molp.2021.07.011

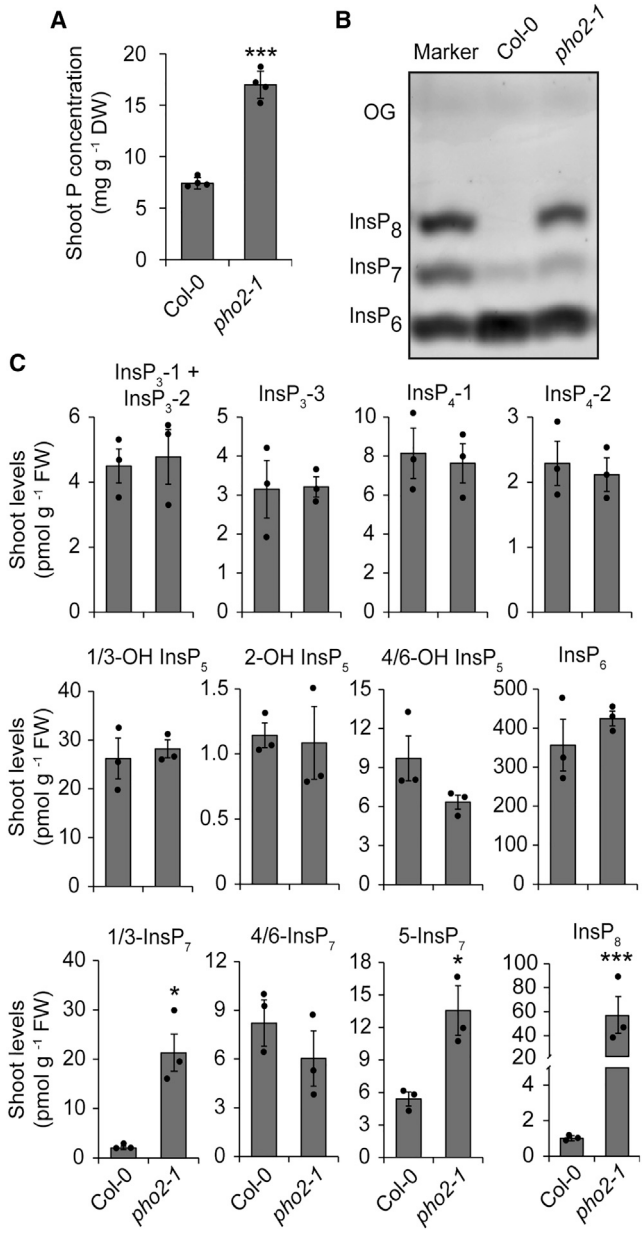

Figure 3. PP-InsPs respond more sensitively to internal P_i status than lower InsPs.

(A) P-overaccumulation phenotype of *pho2-1* plants grown under sufficient P_i conditions in hydroponics. Bars show means ± SD ($n = 4$ biological replicates).

(B and C) PAGE detection **(B)** and CE-ESI-MS analysis **(C)** of inositol (pyro)phosphates in shoots of WT (Col-0) and *pho2-1* plants. OG, orange G. Plants were cultivated in hydroponics under sufficient P_i. Data represent means ± SE ($n = 3$ biological replicates composed of two plants each). $^*P < 0.05$ and $^{***}P < 0.001$, Student's *t*-test.

complemented by reintroducing the genomic *ITPK1* fragment into the mutant background (Supplemental Figure 3), confirming that this defect was indeed associated with the loss of *ITPK1*.

A more detailed analysis with CE-ESI-MS showed that the synthesis specifically of 5-$InsP_7$ is strongly compromised and not any more responsive to P_i in shoots of *itpk1* plants (Figure 4C). This provides the first evidence *in planta* for the ITPK1-dependent generation of 5-$InsP_7$. Loss of *ITPK1* did not significantly affect the levels of the novel 4/6-$InsP_7$ species in shoots (Figure 4C). Despite the strong reduction of 5-$InsP_7$, $InsP_8$ levels were significantly decreased in *itpk1* relative to WT plants only after P_i resupply (Figure 4C). Interestingly, 1/3-$InsP_7$ levels were compromised in *itpk1* and *vih2-4* plants resupplied with P_i. In agreement with HPLC analyses of [^{3}H]inositol-labeled seedlings (Laha et al., 2015), $InsP_8$ levels were strongly decreased in shoots of the *vih2-4* mutant (Figure 4B and 4C). When this mutant was resupplied with P_i, the lower levels of $InsP_8$ were also accompanied by a four-fold increase in 5-$InsP_7$ (Figure 4C). Accumulation of 5-$InsP_7$ increased even further when both *VIH1* and *VIH2* were knocked out (Supplemental Figure 4), providing additional evidence that 5-$InsP_7$ is the main substrate for $InsP_8$ synthesis in shoots.

Apart from an 80% decrease in 5-$InsP_7$, P_i-sufficient *itpk1* plants had also significantly decreased levels of 4/6-OH $InsP_5$ and especially of 1/3-OH $InsP_5$, but increased levels of $InsP_4$-1 and $InsP_3$-3 (Figure 4C). These results are consistent with the catalytic flexibility of inositol 1,3,4-trisphosphate 5/6-kinases (Caddick et al., 2008; Desfougeres et al., 2019; Miller et al., 2005; Whitfield et al., 2020) and provide a detailed quantitative view of the metabolic steps affected by this enzyme *in planta*. Interestingly, the synthesis of even more InsPs, including 2-OH $InsP_5$ and $InsP_6$, was dependent on ITPK1 during P_i resupply (Figure 4C). This result further indicated that a distinct set of reactions occurs in plants experiencing a sudden change in P_i availability compared with those acclimated to P_i-replete conditions. Disruption of *VIH2* resulted in little to no significant change in lower InsP forms (Figure 4C), in line with the substrate specificity of diphosphoinositol pentakisphosphate kinases (Mulugu et al., 2007; Wang et al., 2014a; An et al., 2019).

Together, our results demonstrate that the rapid synthesis of $InsP_8$ in response to P_i is largely dependent on 5-$InsP_7$ synthesized by ITPK1. However, the differences that we detected in plants acclimated to P_i-replete conditions versus those exposed to short-term P_i resupply suggest that compensation mechanisms and metabolic rearrangements might be activated over the long run when ITPK1 or VIH2 activities are perturbed.

ITPK1 has $InsP_6$ kinase and ATP synthase activities

Considering that ITPK1 is required for the robust increase in $InsP_8$ in response to P_i resupply, we asked whether ITPK1 is also able to function as an $InsP_7$ kinase. However, neither 1-$InsP_7$ nor 5-$InsP_7$ appears to be a substrate for ITPK1 kinase activity *in vitro* (Supplemental Figure 5A). Subsequently, the enzymatic properties of recombinant *Arabidopsis* ITPK1 were investigated in more detail with nuclear magnetic resonance spectroscopy (NMR). First, $InsP_6$ kinase reaction conditions were analyzed with respect to magnesium ion (Mg^{2+}) concentration and temperature dependency as well as quenching efficiency of EDTA (Supplemental Figure 5B–5D). Subsequent kinetic analysis revealed that ITPK1 exhibits a surprisingly high K_M for ATP of approximately 520 μM (Figure 5A and 5B). Unlike VIHs (Zhu et al., 2019), the kinase activity of ITPK1 was largely insensitive to P_i and not affected by the non-metabolizable P_i analog phosphite (Supplemental Figure 6). When 2-OH $InsP_5$

Please cite this article in press as: Riemer et al., ITPK1 is an $InsP_6$/ADP phosphotransferase that controls phosphate signaling in *Arabidopsis*, Molecular Plant (2021), https://doi.org/10.1016/j.molp.2021.07.011

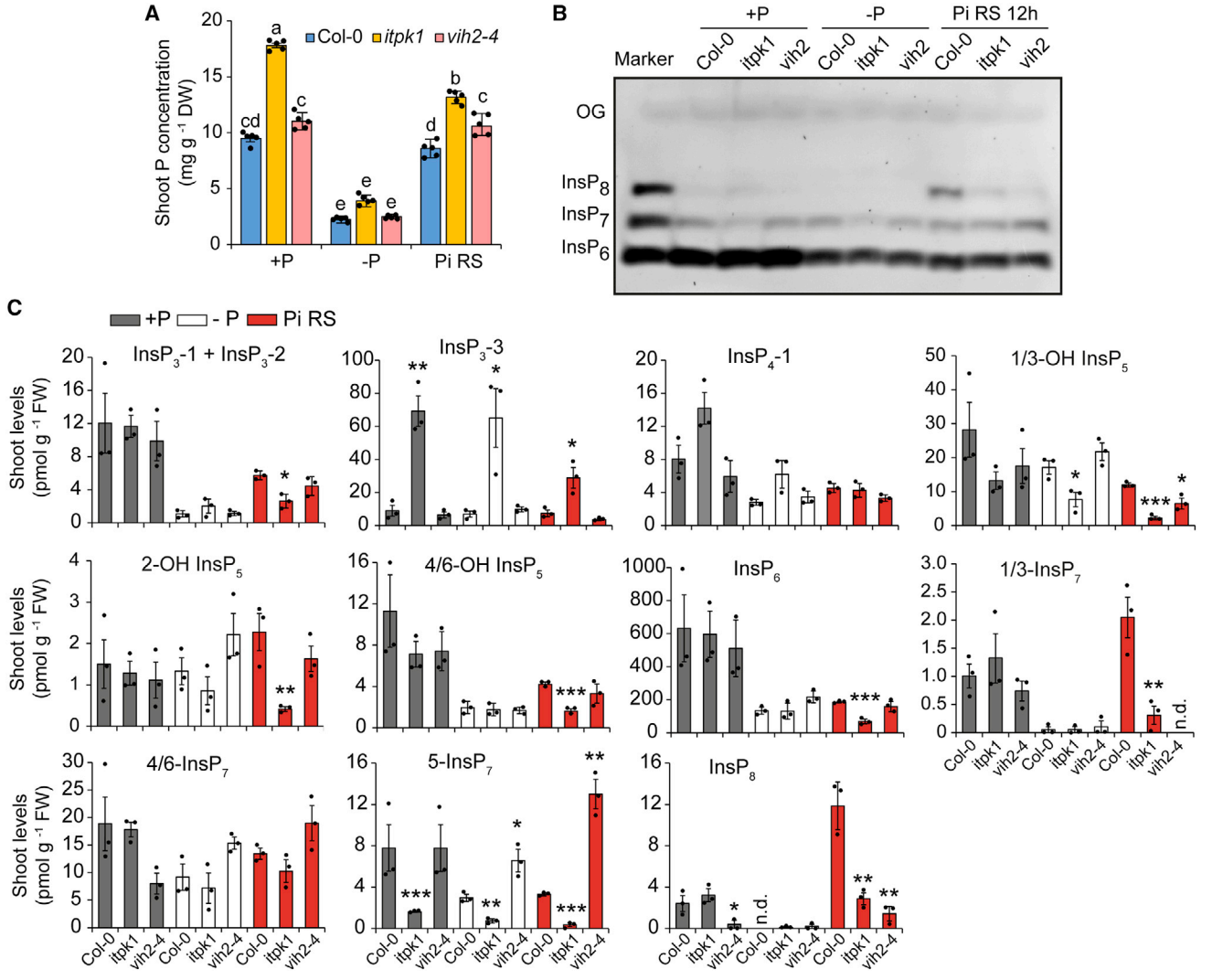

Figure 4. ITPK1 is required for 5-$InsP_7$ synthesis *in planta* and acts with VIH2 to generate $InsP_8$ in response to P_i resupply.
(A) P overaccumulation of *itpk1* plants grown in hydroponics under sufficient P_i (+P), deficient P_i for 7 days (−P), or −P resupplied with P_i for 12 h (Pi RS). Bars show means ± SD (n = 5 biological replicates). Different letters indicate significant differences according to Tukey's test ($P < 0.05$).
(B and C) PAGE detection **(B)** and CE-ESI-MS analysis **(C)** of inositol (pyro)phosphates in shoots of WT (Col-0), *itpk1*, and *vih2-4* plants. OG, orange. Plants were cultivated in hydroponics under sufficient P_i (+P), deficient P_i for 7 days (−P), or −P resupplied with P_i for 12 h (Pi RS). Data represent means ± SE (n = 3 biological replicates). *$P < 0.05$, **$P < 0.01$, and ***$P < 0.001$, Student's t-test (mutant versus Col-0). n.d., not detected.

was presented as substrate to ITPK1, no conversion could be detected (Supplemental Figure 5E), suggesting that ITPK1 has no inositol pentakisphosphate kinase-like activity to generate $InsP_6$ from 2-OH $InsP_5$. Furthermore, in contrast to $InsP_6$ kinases of the IP6K/Kcs1 family, no activity was observed when 1-$InsP_7$ was used as a substrate (Supplemental Figure 5F and 5G), thus confirming our PAGE results from corresponding *in vitro* reactions (Supplemental Figure 5A).

The characterization of structurally and sequence-unrelated mammalian $InsP_6$ kinases of the IP6K family and of ITPK1 from potato has demonstrated that these enzymes can shift their activities from kinase to ADP phosphotransferase at low ATP-to-ADP ratios (Caddick et al., 2008; Voglmaier et al., 1996; Wundenberg et al., 2014). This prompted us to assess if *Arabidopsis* ITPK1 also possesses such activity. *In vitro* reactions with unlabeled 5-$InsP_7$ and subsequent PAGE analyses revealed that ITPK1 indeed mediates 5-$InsP_7$ dephosphorylation (Figure 5C). This activity was recently also reported by Whitfield et al. (2020) and occurred only in the presence of ADP (Supplemental Figure 7A). Interestingly, we found that the ADP phosphotransferase activity of ITPK1 was lost in stable catalytically dead ITPK1 mutants (Figure 5C), indicating that dephosphorylation is mediated by the reverse reaction of the kinase domain and not by a dedicated (albeit cryptic) phosphatase domain. Furthermore, we detected no ADP phosphotransferase activity of ITPK1 with any other $InsP_7$ isomer phosphoryl donor (Figure 5D), suggesting a high degree of substrate specificity for the dephosphorylation reaction. To determine the kinetic parameters of this reaction, we incubated ITPK1 with $^{13}C_6$-labeled 5-$InsP_7$ in the presence of ADP and detected the formation of ATP and $InsP_6$ with NMR (Supplemental Figure 7B and 7C). No ATP formation was detected when ITPK1 was incubated without 5-$InsP_7$ (Supplemental Figure 7D). Interestingly, the reverse reaction was

Please cite this article in press as: Riemer et al., ITPK1 is an $InsP_6$/ADP phosphotransferase that controls phosphate signaling in *Arabidopsis*, Molecular Plant (2021), https://doi.org/10.1016/j.molp.2021.07.011

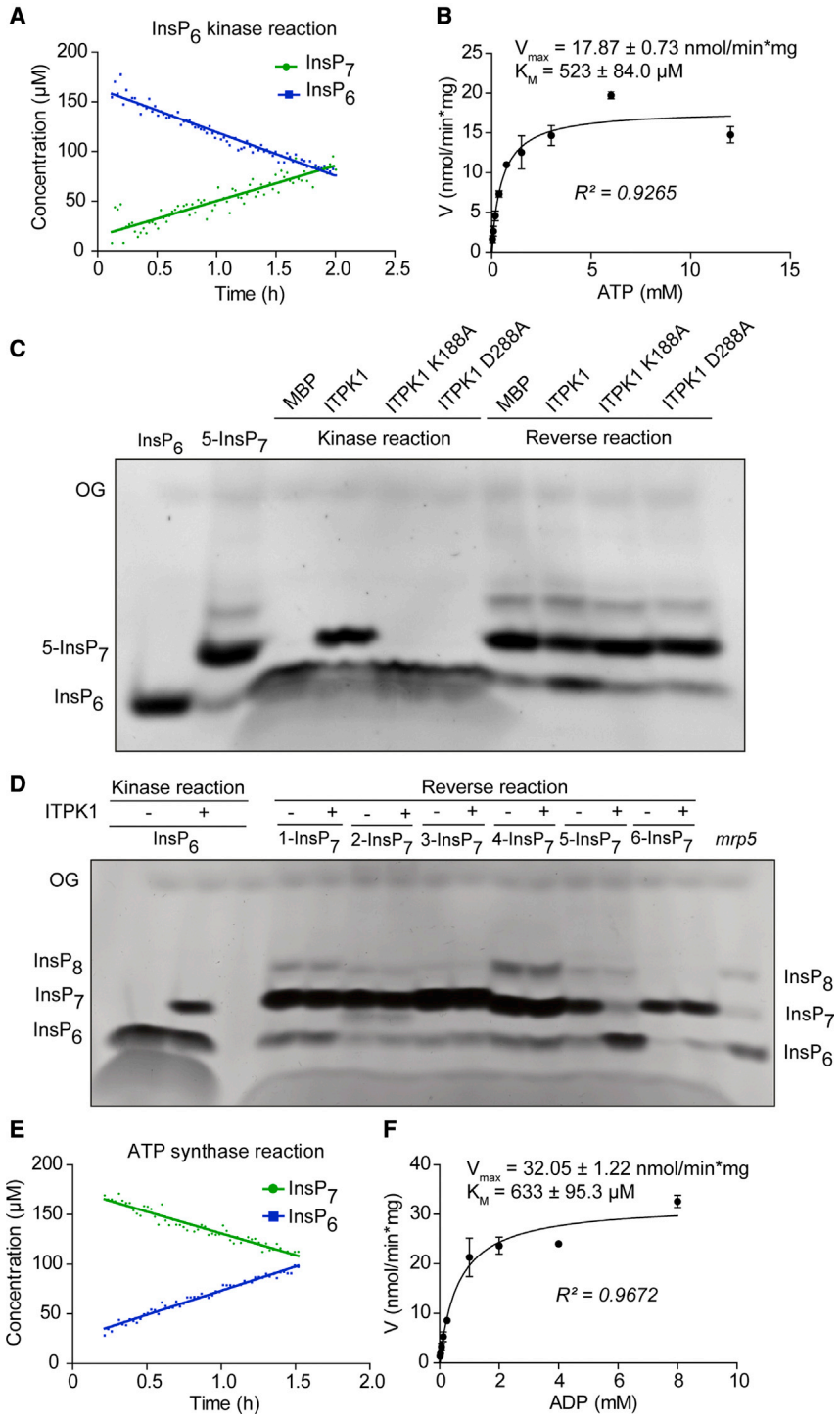

Figure 5. *In vitro* characterization of *Arabidopsis* ITPK1 activity.

(A and B) NMR analysis of $InsP_6$ kinase activity of recombinant *Arabidopsis* ITPK1. Time-dependent conversion of $InsP_6$ to 5-$InsP_7$ **(A)** and reaction velocity determined at varying ATP concentrations **(B)**. K_M and V_{max} were obtained after fitting of the data against the Michaelis-Menten model.

(C and D) $InsP_6$ kinase and 5-$InsP_7$ hydrolysis by recombinant *Arabidopsis* ITPK1 and designated catalytic mutants of ITPK1 **(C)** and specificity of the reverse reaction on 5-$InsP_7$ but not on other $InsP_7$ isomers **(D)**. InsPs were separated via PAGE and visualized by toluidine blue staining. The identity of bands was determined by migration compared with $InsP_6$ and 5-$InsP_7$ standards and TiO_2-purified *mrp5* seed extract. $InsP_6$ kinase reaction served as positive control for the reverse reactions. Purified His_6-MBP tag (MBP) served as negative control for ITPK1.

(E and F) NMR analysis of reverse reaction of recombinant *Arabidopsis* ITPK1. Accumulation of $InsP_6$ and conversion of 5-$InsP_7$ **(E)** and reaction velocity determined at varying ADP concentrations **(F)**. K_M and V_{max} were obtained after fitting of the data against the Michaelis-Menten model.

almost two times faster than the forward, $InsP_6$ kinase, activity, whereas the K_M for ADP and ATP were relatively similar (Figure 5B, 5E, and 5F). In agreement with results obtained in agar-plate-grown seedlings (Zhu et al., 2019), we observed that ATP levels and ATP/ADP ratios dropped significantly in response to P_i deficiency in shoots of hydroponically grown WT plants, but rapidly increased after P_i resupply (Supplemental Figure 8A and 8B). Furthermore, *pho2-1* plants also had higher ATP levels and ATP/ADP ratios than WT (Supplemental Figure 8C and 8D). Thus, the P_i-dependent changes in adenylate nucleotide ratio of plants may ultimately regulate the synthesis of 5-$InsP_7$ by shifting ITPK1-mediated $InsP_6$ kinase and ADP phosphotransferase activities.

ITPK1 is genetically linked to VIH2 and acts redundantly with ITPK2 to maintain P_i homeostasis in *Arabidopsis*

The P_i-overaccumulation phenotype of *itpk1* plants has been associated to the misregulation of PSI genes (Kuo et al., 2018; Supplemental Figure 9A). A full elemental analysis indicated that the concentrations of other nutrients were largely unaffected in shoots of *itpk1* plants (Supplemental Figure 10), demonstrating that the high P levels were not caused by a concentration effect due to the reduced shoot size. In *itpk1* plants, total P levels were also significantly increased in flowers and seeds and slightly increased in roots (Supplemental Figure 9B). A root phenotypical analysis revealed that *itpk1* plants had shorter roots than WT plants irrespective of P_i supply (Supplemental Figure 9C–9E; Laha et al., 2020). This phenotype was probably not due to P_i overaccumulation, as root length of *pho2-1* plants was comparable to that of WT (Supplemental Figure 9F), but likely associated with defective auxin perception (Laha et al., 2020).

To investigate the genetic link between ITPK1 and VIH2, we generated an *itpk1 vih2-4* double mutant. Compared with *itpk1* mutant plants, mutation of *VIH2* in the *itpk1* background

Please cite this article in press as: Riemer et al., ITPK1 is an $InsP_6$/ADP phosphotransferase that controls phosphate signaling in *Arabidopsis*, Molecular Plant (2021), https://doi.org/10.1016/j.molp.2021.07.011

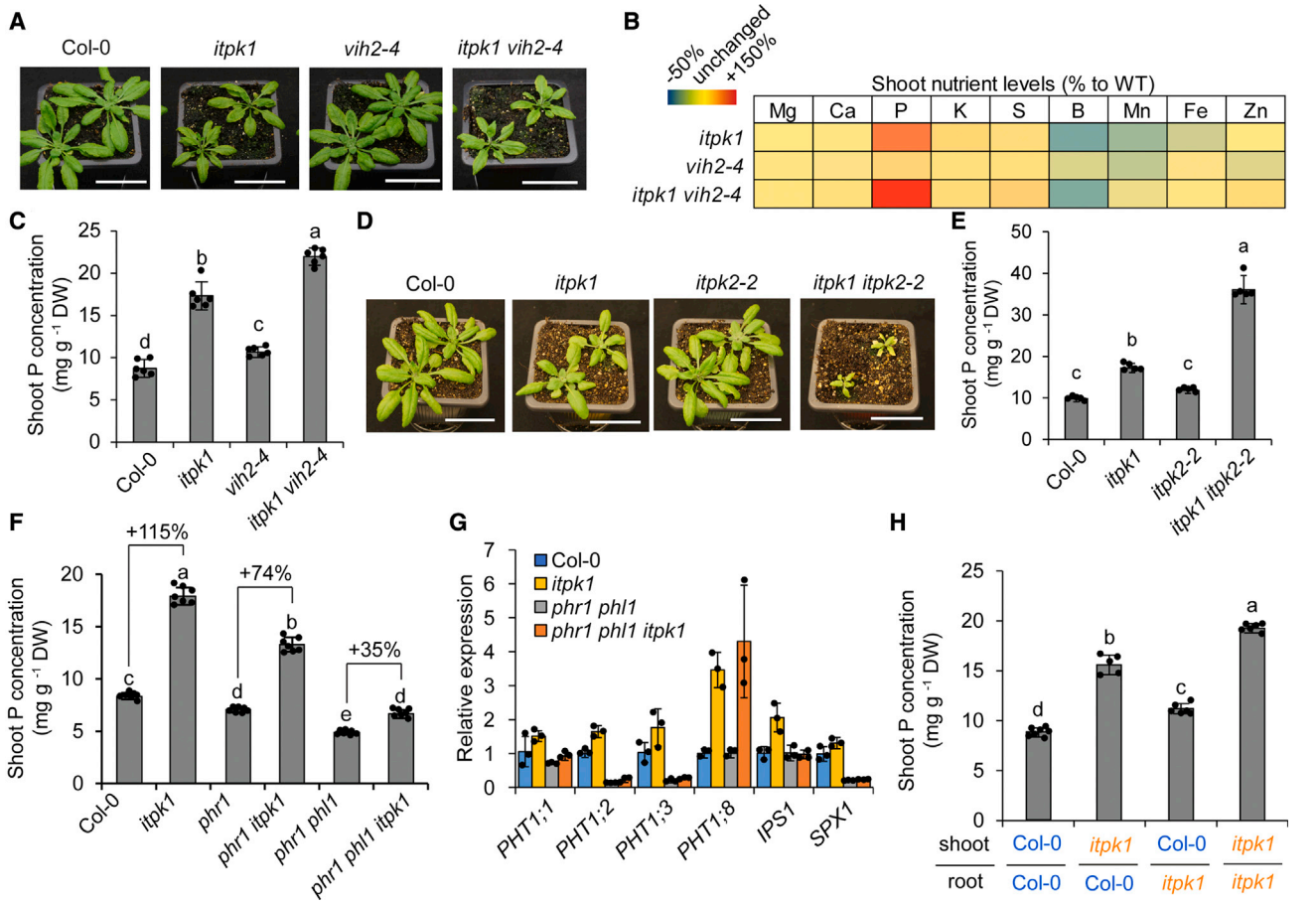

Figure 6. Genetic interaction of ITPK1 with VIH2 and ITPK2 in regulating P_i homeostasis in a PHR1- and PHL1-dependent manner.
(A–C) Characterization of *itpk1 vih2-4* double mutant. Photographs of 4-week-old plants grown on peat-based substrate **(A)**, overview of relative nutrient changes in shoots **(B)**, and shoot P levels **(C)** of wild type (Col-0) and the indicated mutants. Scale bars, 3 cm. Data represent means ± SD (n = 6 plants).
(D and E) Characterization of *itpk1 itpk2-2* double mutant. Photographs of 4-week-old plants grown on peat-based substrate **(D)** and shoot P levels **(E)** of wild type (Col-0) and the indicated mutants. Scale bars, 3 cm. Data represent means ± SD (n = 5 or 6 plants).
(**F and G**) Genetic interplay between PHR1/PHL1 and ITPK1 in systemic P_i signaling. Shoot P levels **(F)** of 3-week-old wild type and indicated mutants grown on peat-based substrate. Data represent means ± SD (n = 6 plants). ITPK1-dependent expression of P_i deficiency-induced genes (**G**) in roots of the indicated P_i-sufficient plants. Data represent means ± SE (n = 3 replicates).
(H) Total P concentration in shoots of self-grafted or reciprocally grafted wild type (Col-0) and *itpk1* grown for 2 weeks on peat-based substrate. Data represent means ± SD (n = 5–7 plants).
In **(C)**, **(E)**, **(F)**, and **(H)**, different letters indicate significant differences according to Tukey's test ($P < 0.05$).

inhibited plant growth even further and caused an approximately 27% increase specifically in shoot P levels (Figure 6A–6C). These results provide genetic evidence for the interdependence of ITPK1 and VIH2 activities to maintain undisturbed P_i homeostasis in plants.

Previously, we demonstrated that ITPK2 also has $InsP_6$ kinase activity *in vitro* (Laha et al., 2019). However, at the phenotypical level, only the disruption of *ITPK1* but not of *ITPK2* results in smaller plant size and constitutive P overaccumulation (Figure 6D and 6E; Kuo et al., 2018). The levels of $InsP_8$, 5-$InsP_7$, and other (pyro)phosphates detected with CE-ESI-MS were mostly unaltered in the *itpk2-2* mutant compared with WT (Supplemental Figure 11). Despite the differential phenotypes of *itpk1* and *itpk2-2* mutants, possible functional redundancy could still explain why *itpk1* plants do not show severe growth and P-overaccumulation phenotypes like those reported for the *vih1 vih2* double mutant (Dong et al., 2019; Zhu et al., 2019). Therefore, we generated an *itpk1 itpk2-2* double mutant. When grown in P_i-containing substrate, *itpk1 itpk2-2* plants exhibited severe growth retardation (Figure 6D). In these plants, shoot P levels were approximately 3.5-fold and 2.1-fold higher than in WT and *itpk1* plants, respectively (Figure 6E). These results suggested that, although ITPK2 plays a relatively minor role in P_i signaling in the presence of a functional ITPK1, it is able to partially compensate for the loss of ITPK1.

ITPK1 controls P_i signaling dependent of PHR1 and PHL1 but independent of PHO2

We then analyzed the genetic interaction between ITPK1 and the transcription factors PHR1 and PHL1. Although *phr1 itpk1* and *phr1 phl1 itpk1* plants still accumulated significantly more P than *phr1* and *phr1 phl1*, respectively, the relative increments were smaller than in the presence of functional PHR1 and PHL1

Please cite this article in press as: Riemer et al., ITPK1 is an $InsP_6$/ADP phosphotransferase that controls phosphate signaling in *Arabidopsis*, Molecular Plant (2021), https://doi.org/10.1016/j.molp.2021.07.011

(Figure 6F). In contrast, the short-root phenotype caused by *ITPK1* disruption could not be restored by knocking out these transcription factors (Supplemental Figure 12A). While many PSI genes were suppressed in the triple mutant, absence of ITPK1 kept *PHT1;8* upregulated in the *phr1 phl1* background (Figure 6G), suggesting that *PHT1;8* expression was further controlled by another mechanism. To investigate whether ITPK1 is also involved in P_i starvation signaling at the level of PHO2, we then generated an *itpk1 pho2-1* double mutant. Knocking out both *ITPK1* and *PHO2* increased shoot P levels by almost two times compared with single *itpk1* and *pho2-1* mutants (Supplemental Figure 12B), hence suggesting that ITPK1 function in P_i signaling is largely independent of PHO2. Collectively, our results demonstrate that the coordination of P_i signaling by PHR1 and PHL1 is tightly linked to ITPK1-dependent PP-InsP synthesis.

We then performed grafting experiments to address whether undisturbed P_i accumulation is determined by organ-specific ITPK1 activity. As expected, shoot P overaccumulation was detected when roots and shoots of *itpk1* plants were self-grafted (Figure 6H). However, shoot P was largely reverted back to WT levels when Col-0 shoots were grafted onto *itpk1* roots, while remaining approximately 75% higher when *itpk1* shoots were grafted onto Col-0 roots. These results suggest that ITPK1 activity in shoots is more determinant for the regulation of shoot P_i accumulation.

Root-specific synthesis of a presumptive novel PP-InsP relies on ITPK1 activity in roots

The apparent dominant ITPK1 role in shoots is puzzling, as *ITPK1* is expressed in various plant tissues, including roots (Kuo et al., 2018). CE-ESI-MS analysis of roots revealed that *itpk1* plants exhibited significantly decreased levels of 1/3-$InsP_7$, 5-$InsP_7$, and $InsP_8$ whenever P_i was available (Supplemental Figure 13). Furthermore, most InsPs that were affected in shoots by *ITPK1* disruption were also affected in roots. Interestingly, PP-InsP levels in roots were lower than those detected in shoots, and the increased accumulation of $InsP_8$ after P_i resupply was less pronounced (compare Figure 4C and Supplemental Figure 13). We therefore compared the levels of PP-InsPs and InsPs in roots and shoots of WT plants and detected clear, organ-specific differences (Figure 7A and 7B). $InsP_8$ and the detected $InsP_7$ isomers were much more abundant in shoots than in roots (Figure 7A). For instance, $InsP_8$ levels in shoots were approximately 2-, 2.4-, and 21-fold higher than those detected in roots of P_i-sufficient, P_i-starved, and P_i-resupplied plants, respectively. Interestingly, the shoot/root ratio was reversed for most InsPs (Figure 7B). While $InsP_6$ levels were comparable in roots and shoots whenever P_i was available, most other InsPs were quantitatively less abundant in shoots than in roots. However, shoot-to-root partitioning of $InsP_4$-1, 2-OH $InsP_5$, and $InsP_6$ was increased under P_i starvation, as their synthesis was inhibited more strongly in roots than in shoots. Thus, these results demonstrate strong, organ-specific differences in InsP and PP-InsP metabolism, with higher levels of PP-InsPs produced in shoots and lower InsPs in roots.

Notably, PAGE analyses of root samples revealed a P_i-deficiency-induced accumulation of a band with an electrophoretic mobility between those of $InsP_6$ and $InsP_7$, which was absent in shoots (Figure 7C; Supplemental Figure 14A). With CE-ESI-MS we identified the presence of an isomer that, to our knowledge, has not previously been reported in plants. This isomer displayed a mobility slightly increased compared with $InsP_6$, thus likely representing a PP-$InsP_4$ isomer (Supplemental Figure 14B). We were not yet able to determine the isomeric nature of this presumptive PP-$InsP_4$ isomer, but observed that it did not co-migrate with synthetic 5PP-Ins(1,3,4,6)P_4. We also detected a band with a similar mobility in roots of rice plants (Supplemental Figure 14B). CE-ESI-MS analyses of individual and mixed samples revealed that the presumptive PP-$InsP_4$ isomer appears to be indistinguishable between *Arabidopsis* and rice roots, but clearly differed in mobility from the 5PP-Ins(1,3,4,6)P_4 standard (Supplemental Figure 14B), suggesting that its root-specific synthesis is conserved in flowering plants. Interestingly, in *Arabidopsis* roots, the levels of this PP-$InsP_4$ isomer were detected only in P_i-starved roots (Figure 7D). In roots of *itpk1* plants, a band representing the presumptive PP-$InsP_4$ was not visible, and the isomer was either not detected or present at lower levels than in WT or *itpk2-2* according to CE-ESI-MS (Figure 7C and 7D), suggesting that ITPK1 is involved in its synthesis. These results together indicate that ITPK1 is active in roots, where it is also required for the root-specific synthesis of a presumptive novel PP-$InsP_4$ isomer.

Subcellular $InsP_6$ compartmentalization determines tissue levels of $InsP_7$ and $InsP_8$

Since roots and shoots had comparable $InsP_6$ levels as long as P_i was available to the plants (Figure 7B), we next addressed whether subcellular compartmentalization of $InsP_6$ could determine the amount of $InsP_7$ and $InsP_8$ that can be synthesized in each plant organ. To this end, we assessed these PP-InsPs in shoots and roots of *mrp5*, a mutant defective in vacuolar loading of $InsP_6$ (Nagy et al., 2009). Compared with WT, *mrp5* plants had elevated $InsP_7$ and $InsP_8$ signals in shoots and roots (Figure 7E). We then quantified these changes in shoots with CE-ESI-MS and found that $InsP_8$ especially was still responsive to P_i in *mrp5* plants (Supplemental Figure 15A). Consequently, P accumulation was not significantly altered (Supplemental Figure 15B), suggesting that P_i starvation responses were not misregulated in *mrp5* mutant plants. Taken together, these results indicate that the amount of PP-InsPs produced in different plant tissues is dependent on MRP5-mediated $InsP_6$ compartmentalization, while the composition may be further determined by organ-specific ITPK1 activities.

DISCUSSION

ITPK1 reversible reactions are important for the formation and degradation of PP-InsPs in response to P_i

Regulation of cellular P_i homeostasis is critical for all living organisms. Therefore, it is not surprising that intricate P_i sensing and signaling mechanisms have evolved to dynamically adjust P_i uptake according to external and internal P_i levels. In plants, recent studies have raised compelling evidence that PP-InsPs act as signaling molecules that regulate P_i homeostasis by binding to SPX proteins (Azevedo and Saiardi, 2017; Dong et al., 2019; Ried et al., 2021; Wild et al., 2016; Zhu et al., 2019). However, it has remained challenging to establish which PP-InsP species are regulated by P_i and to link defects in P_i signaling to altered

Please cite this article in press as: Riemer et al., ITPK1 is an $InsP_6$/ADP phosphotransferase that controls phosphate signaling in *Arabidopsis*, Molecular Plant (2021), https://doi.org/10.1016/j.molp.2021.07.011

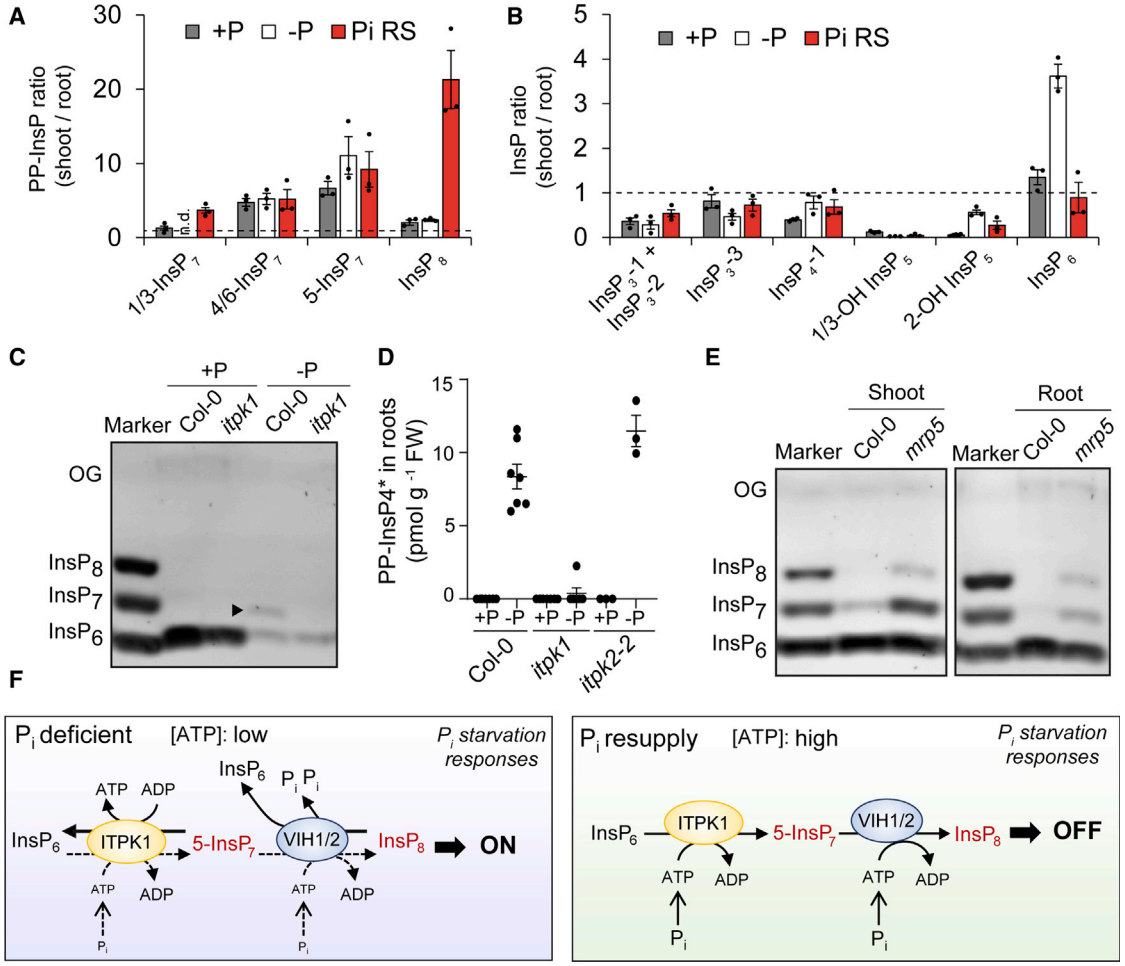

Figure 7. Amount of $InsP_7$ and $InsP_8$ synthesized in plant tissues relies on MRP5-dependent $InsP_6$ compartmentalization and ITPK1 activity.

(A and B) Relative levels of PP-InsPs **(A)** and InsPs **(B)** detected by CE-ESI-MS in shoots and roots of WT (Col-0) plants exposed to variable P_i supplies. Plants were cultivated in hydroponics under sufficient P_i (+P), deficient P_i for 7 days (−P), or −P resupplied with P_i for 12 h (Pi RS). Data are means of shoot-to-root ratios ± SE (n = 3 biological replicates composed of two plants each). n.d., not detected. Dashed lines indicate a ratio of 1.

(C and D) PAGE detection **(C)** and CE-ESI-MS quantification **(D)** of a presumptive novel PP-$InsP_4$ isomer in roots. This isomer was detected in roots of WT (Col-0) or *itpk2-2* plants but was absent or present at low levels in roots of the *itpk1* mutant. Plants were grown in hydroponics in P_i-sufficient solution (+P) or exposed for 7 days to P_i starvation (−P). In **(D)**, data represent means ± SE (n = 6 or 7 biological replicates). Data points set to 0 indicate independent biological replicates in which the isomer was not detected.

(E) PAGE detection of InsPs and PP-InsPs in shoots and roots of WT (Col-0) and *mrp5* mutant plants cultivated in hydroponics under sufficient P_i (+P). Data represent means ± SE (n = 3 biological replicates). OG, orange G.

(F) A proposed model for ITPK1-dependent generation and removal of 5-$InsP_7$ and its link with VIHs and P_i signaling. In P_i-deficient cells, low ATP levels stimulate ITPK1 to catalyze P_i transfer from 5-$InsP_7$ to ADP, thereby generating ATP and decreasing 5-$InsP_7$. Decreased ATP and P_i levels also activate the pyrophosphatase activity of VIHs to break down $InsP_8$. The removal of PP-InsPs destabilizes the association between PHRs and SPXs, allowing PHRs to switch on P_i starvation responses. When cells regain sufficient P_i, which increases ATP levels, ITPK1-mediated $InsP_6$ kinase activity is stimulated and the reverse reaction toward 5-$InsP_7$ is inhibited. 5-$InsP_7$ generated by ITPK1 serves then as substrate for $InsP_8$ production via the kinase domain of VIHs. As a consequence of increased PP-InsPs, SPX proteins recruit PHRs to repress P_i starvation responses. Our results also demonstrate that the amount of PP-InsPs produced in different plant tissues is further controlled by $InsP_6$ compartmentalization by MRP5, and that ITPK2 is able to partially complement ITPK1 function in P_i signaling.

accumulation of specific InsPs in metabolic mutants. With the help of CE-ESI-MS, we show here that 1/3-$InsP_7$, 5-$InsP_7$, and $InsP_8$ levels change dramatically not only when plants are exposed to P_i-limited conditions, but especially when P_i-starved plants are resupplied with P_i (Figures 1A–1G and 2). $InsP_8$, which co-migrated with a [$^{13}C_6$]1,5-$InsP_8$ standard (Figure 2C), responded more sensitively to P_i than any other PP-InsP or lower InsP assessed in this study, with concentrations increasing from approximately 0.32% of $InsP_6$ in shoots of P_i-starved plants to approximately 10% of $InsP_6$ 48 h after P_i resupply (Figure 2D). Due to the severe P_i signaling defects of *vih1 vih2* double mutants and the fact that 1,5-$InsP_8$ can restore SPX1–PHR1 interaction *in vivo* more efficiently than 5-$InsP_7$ (Dong et al., 2019; Zhu et al., 2019; Ried et al., 2021), $InsP_8$ has been suggested as the preferred ligand for SPX proteins. Notably, in contrast to $InsP_8$ accumulation, the expression of *SPX1* and

Please cite this article in press as: Riemer et al., ITPK1 is an $InsP_6$/ADP phosphotransferase that controls phosphate signaling in *Arabidopsis*, Molecular Plant (2021), https://doi.org/10.1016/j.molp.2021.07.011

SPX3 is strongly induced by P_i starvation (Duan et al., 2008). These seemingly opposing responses suggest that when P_i-deficient plants regain access to P_i, the increased accumulation of $InsP_8$ shortly overlaps with the high abundance of its receptors, allowing the quick formation of large amounts of repressive SPX–PHR complexes. As soon as 6 h after P_i resupply, when $InsP_8$ levels were elevated substantially (Figure 2D), the expression of PSI genes in roots was already strongly repressed compared with P_i-starved plants (Supplemental Table 1). Such a mechanism might thereby help plants to efficiently modulate P_i uptake according to the severity of P_i deficiency, thus preventing toxicity after P_i-starved plants regain access to P_i.

Since $InsP_8$ is generated in plants by phosphorylation of $InsP_7$ via VIH1 and VIH2 (Dong et al., 2019; Laha et al., 2015; Zhu et al., 2019), P_i-dependent $InsP_8$ synthesis relies on the availability of the substrate, $InsP_7$. Previous analyses with PAGE or [^{32}P]P_i labeling indicated that $InsP_7$ levels were relatively unchanged or mildly increased in the shoots of P_i-starved plants (Dong et al., 2019; Kuo et al., 2018). In our study we observed, under slightly different conditions, a mild global reduction in $InsP_7$ levels in response to P_i starvation and a quick recovery when P_i was resupplied to plants (Figures 1, 2, 3, and 4). However, this picture became much clearer when employing CE-ESI-MS, which enabled us to distinguish several different $InsP_7$ species. We found that, similar to $InsP_8$, both 5-$InsP_7$ and 1/3-$InsP_7$ were strongly reduced under P_i starvation and recovered quickly after P_i resupply (Figure 2D). Recovery of 1/3-$InsP_7$ was dependent on functional ITPK1 and VIH2. Previous NMR assays showed that the recombinant kinase domain of *Arabidopsis* VIH2 catalyzes the synthesis of $InsP_8$ from 5-$InsP_7$ and of 1-$InsP_7$ from $InsP_6$ (Zhu et al., 2019). Thus, the lack of 1/3-$InsP_7$ in P_i-resupplied *vih2-4* plants provides first support *in planta* for the $InsP_6$ kinase activity of VIH2. Nonetheless, the concomitant increase in 5-$InsP_7$ in shoots of *vih2-4* plants (Figure 4C) indicated that 5-$InsP_7$ is the main VIH2 substrate responsible for the robust $InsP_8$ synthesis induced by P_i resupply in WT plants. In line with the *in vitro* activity of ITPK1 (Adepoju et al., 2019; Laha et al., 2019), shoot 5-$InsP_7$ levels were strongly decreased in *itpk1* mutant plants irrespective of P_i availability (Figure 4C). Since we detected only $InsP_6$ kinase and no 1-$InsP_7$ or 5-$InsP_7$ kinase activity with purified recombinant *Arabidopsis* ITPK1 (Supplemental Figure 5A), the decrease in $InsP_8$ in P_i-resupplied *itpk1* plants likely results from diminished 5-$InsP_7$ and thus reduced availability of this $InsP_7$ isomer for the VIH1- or VIH2-catalyzed phosphorylation at the C1 phosphate. Notably, disruption of *ITPK1* or *VIH2* resulted in distinct changes in a number of inositol (pyro)phosphates in plants acclimated to sufficient P_i compared with plants exposed to short-term P_i resupply (Figure 4C), which could point to time-dependent activation of metabolic readjustments and compensatory mechanisms. Indeed, the phenotypical analysis of an *itpk1 itpk2-2* double mutant provided evidence that ITPK2 is able to partially complement the function of an absent ITPK1 (Figure 6D and 6E). However, future research will have to assess PP-InsPs at higher tissue resolution and in different cellular compartments to determine if the $InsP_8$ detected in shoots of *itpk1* plants acclimated to P_i-replete conditions is produced at the sites relevant for P_i signaling.

The dynamic changes in 1/3-$InsP_7$, 5-$InsP_7$, and $InsP_8$ levels according to the plant's P_i status indicate that PP-InsP synthesis and degradation must be tightly controlled. P_i-dependent accumulation of $InsP_8$ has been proposed to rely on the bifunctional activity of VIH1 and VIH2 (Dong et al., 2019; Zhu et al., 2019), whose kinase and phosphatase activities can be shifted according to cellular ATP and P_i levels (Zhu et al., 2019). However, unlike VIHs, ITPK1 harbors only the atypical "ATP-grasp fold" and no phosphatase domain. Nonetheless, we demonstrate that *Arabidopsis* ITPK1 can shift its activity and become an ADP phosphotransferase that dephosphorylates 5-$InsP_7$ but no other $InsP_7$ isomer in the presence of ADP (Figure 5C–5F and Supplemental Figure 7). Considering that 5-$InsP_7$ represents only one of at least three different $InsP_7$ isomers detected in plants, this high specificity suggests that the reverse reaction is most likely used to specifically switch off 5-$InsP_7$ signaling (and in consequence $InsP_8$ signaling) and probably makes no major contribution to global ATP synthesis under P_i-deficient conditions. Thus, ITPK1 can mediate reversible $InsP_6$ kinase and 5-$InsP_7$ dephosphorylation, which is reminiscent of the Ins(1,3,4,5,6)P_5/ADP phosphotransferase activities recorded previously for recombinant ITPK1 from potato (Caddick et al., 2008). Our kinetic analyses with NMR also demonstrate that *Arabidopsis* ITPK1 has comparable K_M values for ATP and ADP (Figure 5). Thus, P_i-dependent (and perhaps tissue-dependent) changes in ATP levels and ATP/ADP ratios will determine whether ITPK1 phosphorylates $InsP_6$ or dephosphorylates 5-$InsP_7$ to produce or remove PP-InsPs required for undisturbed P_i signaling (Figure 7F). The ADP phosphotransferase activity of ITPK1 could bypass the requirement for dedicated PP-InsP hydrolases, which are likely to slow down quick dynamic changes in $InsP_7$ and $InsP_8$ to induce, e.g., jasmonate-related responses during wound response or insect attack (Laha et al., 2015, 2016), or when P_i becomes suddenly available (Figures 1B–1D and 2D). During the completion of the present study, Whitfield and colleagues (Whitfield et al., 2020) reported that, in addition to 5-$InsP_7$, *Arabidopsis* ITPK1 can also dephosphorylate Ins(1,3,4,5,6)P_5 at high ADP/ATP ratios. Thus, the catalytic flexibility of ITPK1 and its ability to mediate adenylate charge-dependent forward and reverse reactions at different steps along the metabolic pathway make ITPK1 a central component that transduces cellular P_i status into specific inositol (pyro)phosphate changes.

ITPK1 activity in shoots is critical for undisturbed P_i signaling

With genetic crossings and grafting, we demonstrated that the uncontrolled P_i accumulation and misregulated expression of PSI genes in the *itpk1* mutant was strongly attenuated in the absence of PHR1 and PHL1 and was more significantly affected by missing ITPK1 activity in shoots (Figure 6F–6H). The latter result is somewhat surprising, since *ITPK1*, *VIH1*, and *VIH2* are expressed in shoots and roots (Kuo et al., 2014, 2018; Laha et al., 2015; Zhu et al., 2019) and ITPK1 activity also affects PP-InsP accumulation in roots (Supplemental Figure 13). One possibility is that the disturbed PHR-dependent P_i signaling in *itpk1* shoots further amplifies PHR-dependent P_i signaling defects in roots. Furthermore, in line with earlier indications from [^{32}P]P_i labeling (Kuo et al., 2018), we found that the concentration of all PP-InsPs—except for a presumptive novel PP-$InsP_4$ isomer—was higher in shoots than in roots (Figure 7A–7D and Supplemental Figure 14A). Future studies are required to investigate the relevance of these differences for

Please cite this article in press as: Riemer et al., ITPK1 is an $InsP_6$/ADP phosphotransferase that controls phosphate signaling in *Arabidopsis*, Molecular Plant (2021), https://doi.org/10.1016/j.molp.2021.07.011

whole-plant P_i homeostasis. Interestingly, our results indicated that subcellular compartmentalization of $InsP_6$ seems determinant for the overall level of $InsP_6$-dependent PP-InsPs that can be produced in different plant tissues (Figure 7E and Supplemental Figure 15A), while the composition is likely defined by the predominant catalytic activity executed by different enzymes according to substrate availability and the energetic state of each tissue.

Identification of novel PP-InsPs in plants

One surprising finding from our CE-ESI-MS analysis was the identification of a previously unreported 4/6-$InsP_7$ isomer, which, together with 5-$InsP_7$, appears to be the most abundant $InsP_7$ isomer in plants (Figure 2D and Supplemental Figure 2). The 4/6-$InsP_7$ isomer is not misregulated in the *pho2* mutant and does not show the strong overshoot reaction observed for 1/3-$InsP_7$ and $InsP_8$ after P_i resupply and is hence likely not involved in P_i signaling (Figures 2D and 3C). Neither 4-$InsP_7$ nor 6-$InsP_7$ has been described, to our knowledge, in other organisms, with the exception of the social amoeba *Dictyostelium discoideum*, in which 6-$InsP_7$ represents the most abundant $InsP_7$ isomer (Laussmann et al., 1997). The amounts of $InsP_7$ and $InsP_8$ are very high in *Dictyostelium*, reaching concentrations of several hundred millimolar (Wilson et al., 2015). Their synthesis is required for chemotactic responses and depends on an $InsP_6$ kinase related to mammalian IP6Ks (Luo et al., 2003). We therefore hypothesize that 4/6-$InsP_7$ synthesis in plants and *Dictyostelium* might have evolved differently, and additional experiments will be required to determine the exact isomeric nature of this species.

We also identified a root-specific, ITPK1-dependent PP-$InsP_4$ isomer that is regulated by P_i availability but is distinct from the known 5PP-Ins(1,3,4,6)P_4 isomer (Figure 7C and 7D; Supplemental Figure 14) that appears to accumulate in the yeast *ipk1* mutant (Draskovic et al., 2008). Interestingly, a recent study showed that recombinant ITPK1 is able to phosphorylate Ins(1,2,3,4,5)P_5, but none of the other simple $InsP_5$ isomers (Whitfield et al., 2020), possibly explaining the synthesis of this unknown PP-$InsP_4$ in roots. Future work is necessary to reveal the structure of this isomer and whether it potentially also binds to SPX domains, and to assess if the strict organ-specific and P_i-dependent accumulation of this presumptive PP-$InsP_4$ isomer is involved in P_i signaling.

METHODS

Plant materials and growth conditions

Seeds of *A. thaliana* T-DNA insertion lines *itpk1* (SAIL_65_D03), *itpk2-2* (SAIL_1182_E03), *vih2-4* (GK-080A07), *mrp5* (GK-068B10), *pho2-1* (ethyl methanesulfonate mutant described in Delhaize and Randall, 1995), and *phr1* (SALK_067629) were obtained from The European *Arabidopsis* Stock Centre (http://arabidopsis.info/). The *phr1 phl1* double mutant and the *phr1 phl1 vih1 vih2* quadruple mutant used in this study were described previously (Kuo et al., 2014; Zhu et al., 2019). To generate the *phr1 itpk1* double and the *phr1 phl1 itpk1* triple mutant, we crossed *itpk1* with, respectively, *phr1* and the homozygous *phr1 phl1* mutant. The double mutants *itpk1 itpk2-2*, *itpk1 pho2-1*, and *itpk1 vih2-4* were generated by crossing the respective single homozygous mutants. F2 and F3 plants were genotyped by PCR using the primers indicated in Supplemental Table 2 to identify homozygous lines. The homozygous *pho2-1* allele was confirmed by sequencing. Transgenic lines expressing the genomic *ITPK1* fragment in the *itpk1* background were generated as described in Laha et al. (2020).

To investigate P_i-dependent regulation of inositol (pyro)phosphate metabolism with PAGE and CE-ESI-MS, *Arabidopsis* and rice plants were grown in hydroponics as described in detail in the supplemental methods. *P. patens* was grown on Knop medium (Reski and Abel, 1985) solidified with 0.8% agar (A7921, Sigma). Light was provided by fluorescent lamps (60 μmol m^{-2} s^{-1}) under a regime of 16 h light and 8 h darkness at constant 20°C. P_i treatments were achieved by transferring pre-cultivated plants to fresh Knop solid medium containing 1.8 mM KH_2PO_4 (+P) or 1.8 mM KCl (−P) for 30 days. At the end of P_i starvation period, some of the plants were resupplied with 1.8 mM KH_2PO_4 and harvested after 24 h or 96 h.

Phenotypic characterization of *Arabidopsis* WT and mutants in soil substrate was performed by germinating seeds directly in pots filled with peat-based substrate (Klasmann-Deilmann GmbH, Germany). The pots were placed inside a conditioned growth chamber with a 22°C/18°C and 16-h/8-h light/dark regime at a light intensity of 120 μmol photons m^{-2} s^{-1} supplied by fluorescent lamps. Plants were bottom watered at regular intervals. Seedlings were thinned after 1 week to leave only two plants per pot. Whole shoots or different plant parts were harvested as indicated in the legend of figures.

Cultivation of HCT116 cells

Mammalian cells were cultivated as described (Wilson et al., 2015). Briefly, HCT116 cells were grown in DMEM medium supplemented with 10% fetal bovine serum and 0.45% glucose in a humidified atmosphere with 5% CO_2. P_i starvation was induced with DMEM without sodium phosphate supplemented with 10% dialyzed fetal bovine serum. Cells were washed twice in the phosphate-free medium before incubation with DMEM medium with or without phosphate. Analysis of InsPs from HCT116 cell lines was performed as previously described (Wilson et al., 2015).

Grafting experiment

Collar-free grafting was performed exactly as described in Rus et al. (2006). Successfully grafted seedlings were transplanted directly to peat-based soil and whole shoots harvested for elemental analysis 2 weeks later.

RNA isolation and quantitative real-time PCR

Root and shoot tissues were collected by excision and immediately frozen in liquid N_2. Total RNA was extracted with the RNeasy Plant Mini Kit (Macherey-Nagel, Germany). Quantitative reverse transcriptase PCR was conducted with the CFX384TM real-time system (Bio-Rad, Germany) and Go Taq qPCR Master Mix SybrGreen I (Promega) using the primers listed in Supplemental Table 2. *UBQ2* was used as a reference gene to normalize relative expression levels of all tested genes. Relative expression was calculated according to Pfaffl (2001).

Elemental analysis

Whole shoots were dried at 65°C and digested in concentrated HNO_3 in polytetrafluoroethylene tubes under a pressurized system (UltraCLAVE IV, MLS). Elemental analysis of plant samples from hydroponics or pot experiments was performed by inductively coupled plasma optical emission spectrometry (iCAP 700, Thermo Fisher Scientific), whereas *P. patens* samples were analyzed by sector field high-resolution inductively coupled plasma–MS (ELEMENT 2, Thermo Fisher Scientific). Element standards were prepared from certified reference materials from CPI International.

Titanium dioxide bead extraction and PAGE

All steps until dilution were performed at 4°C. TiO_2 beads (titanium(IV) oxide rutile, Sigma Aldrich) were weighted to 10 mg for each sample and washed once in water and once in 1 M perchloric acid (PA). Liquid-N_2-frozen plant

Please cite this article in press as: Riemer et al., ITPK1 is an $InsP_6$/ADP phosphotransferase that controls phosphate signaling in *Arabidopsis*, Molecular Plant (2021), https://doi.org/10.1016/j.molp.2021.07.011

material was homogenized using a pestle and immediately resuspended in 800 μl ice-cold PA. Samples were kept on ice for 10 min with short intermediate vortexing and then centrifuged for 10 min at 20 000 *g* at 4°C using a refrigerated benchtop centrifuge. The supernatants were transferred into fresh 1.5-ml tubes and centrifuged again for 10 min at 20 000 *g*. To absorb InsPs onto the beads, the supernatants were resuspended in the pre-washed TiO_2 beads and rotated at 4°C for 30–60 min. Afterward, the beads were pelleted by centrifuging at 8000 *g* for 1 min and washed twice in PA. The supernatants were discarded. To elute inositol polyphosphates, beads were resuspended in 200 μl 10% ammonium hydroxide and then rotated for 5 min at room temperature. After centrifuging, the supernatants were transferred into fresh 1.5-ml tubes. The elution process was repeated and the second supernatants were added to the first. Eluted samples were vacuum evaporated at 45°C to dry completely. InsPs were resuspended in 20 μl ultrapure water and separated by 33% PAGE and visualized by toluidine blue staining, followed by 4′,6-diamidino-2-phenylindole staining based on previously established protocols (Losito et al., 2009; Wilson et al., 2015; Wilson and Saiardi, 2018). Signal intensities of PAGE were quantified with ImageJ.

CE-ESI-MS/MS

CE-ESI-MS/MS was performed on an Agilent 7100 CE system directly interfaced with a triple-quadrupole tandem MS Agilent 6495c system, equipped with an Agilent Jet Stream ESI source. CE-MS coupling was carried out using a sheath liquid coaxial interface, with an Agilent 1200 isocratic LC pump constantly delivering the sheath liquid (via a splitter set with a ratio of 1:100). Agilent MassHunter Workstation (version 10.1) was employed to control the entire system, data acquisition, and analysis. All experiments were performed with a bare fused silica capillary with a length of 100 cm and 50 μm internal diameter. Forty millimolar ammonium acetate titrated by ammonia solution to pH 9.0 was used as background electrolyte. Before the first use, the capillary was conditioned by rinsing with 1 M sodium hydroxide (10 min), water (10 min), and background electrolyte (20 min). A constant CE current of 27 μA was established by applying +30 kV over the capillary. Five microliters of InsP extracts from TiO_2 purification were mixed with 5 μl isotopic standards mixture (Puschmann et al., 2019; 4 μM [$^{13}C_6$]1,5-$InsP_8$, 4 μM [$^{13}C_6$]5-$InsP_7$, 4 μM [$^{13}C_6$]1-$InsP_7$, 40 μM [$^{13}C_6$]$InsP_6$, and 8 μM [$^{13}C_6$]2-OH $InsP_5$). Samples were injected by applying 100 mbar pressure for 10 s (20 nl). In some cases, 35 mM ammonium acetate titrated by ammonia solution to pH 9.7 was used for a second measurement for the quantitation of 1/3-$InsP_7$ and 2-OH $InsP_5$. The sheath liquid was composed of a water–isopropanol (1:1) mixture, which was introduced at a flow rate of 10 μl/min. The MS source parameters setting with respect to the sensitivity and stability were as follows: nebulizer pressure was 8 psi, gas temperature was 150°C, and with a flow of 11 l/min, sheath gas temperature was 175°C, and with a flow at 8 l/min, the capillary voltage was −2000 V with nozzle voltage 2000 V. Negative high-pressure RF and low-pressure RF (ion funnel parameters) were 70 V and 40 V, respectively. Mass spectrometer parameters for MRM transitions are shown below, and were identified by MassHunter Optimizer software. Mass spectrometer parameters for the analysis of InsPs are shown in Supplemental Table 3. $InsP_8$, 5-$InsP_7$, 1/3-$InsP_7$, $InsP_6$, and 2-OH $InsP_5$ were assigned by MS/MS transitions and identical migration time compared with their heavy isotopic reference. 4/6-$InsP_7$, 4/6-OH $InsP_5$, and 1/3-OH $InsP_5$ were identified by MS/MS transition and same migration time compared with relative standards. Three $InsP_3$ and two $InsP_4$ isomers were assigned by MS/MS transitions and based on a comparison with results of [^{3}H]inositol HPLC labeling experiments. Quantification of $InsP_8$, 5-$InsP_7$, 1/3-$InsP_7$, $InsP_6$, and 2-OH $InsP_5$ was performed with known amounts of corresponding heavy isotopic references spiked into the samples. Due to the close migration, [$^{13}C_6$]5-$InsP_7$ was employed as internal standard for 4/6-$InsP_7$, [$^{13}C_6$]2-OH $InsP_5$ was taken as internal standard for 4/6-OH $InsP_5$, 1/3-OH $InsP_5$, $InsP_4$s and $InsP_3$s..

ITPK1 *in vitro* kinase and ATP synthase assay

Recombinant *A. thaliana* ITPK1 was purified based on the previously established protocol (Schaaf et al., 2006). The $InsP_6$ kinase assay was performed by incubating 10.17 μM enzyme in a reaction mixture containing 5 mM $MgCl_2$, 20 mM HEPES (pH 7.5), 1 mM DTT, 5 mM phosphocreatine, 0.33 units creatine kinase, 12.5 mM ATP, and 1 mM $InsP_6$ (Sichem) at 25°C for 6 h. The ability of the enzyme to dephosphorylate 5-$InsP_7$ was assayed in a reaction mixture containing 3 μg enzyme, 2.5 mM $MgCl_2$, 50 mM NaCl, 20 mM HEPES (pH 6.8), 1 mM DTT, 1 mg/ml BSA, 8 mM ADP, and 1 mM 5-$InsP_7$ at 25°C for 6 h. Reactions were separated by 33% PAGE and visualized by toluidine blue staining.

NMR-based enzyme assays

Full-length recombinant *A. thaliana* ITPK1 in H_2O was used in all assays. ITPK1 (0.2–0.8 μM) was incubated in reaction buffer containing 20 mM HEPES (pH 7.0, measured in D_2O), 50 mM NaCl, 1 mM DTT, 5 mM creatine phosphate, 1 U/ml creatine kinase, 2.5 mM $MgCl_2$ (if not indicated otherwise), and 175 μM [$^{13}C_6$]$InsP_5$ [2-OH], [$^{13}C_6$]$InsP_6$, [$^{13}C_6$]5-$InsP_7$, or [$^{13}C_6$]1-$InsP_7$ in D_2O. If not indicated otherwise, the reaction buffer also included 2.5 mM ATP or 2.5 mM ADP.

For single timepoint analysis of enzyme activity, 2.25–0.375 ng (0.2–0.3 μM) ITPK1 was used. Reactions (150 μl) were incubated at 25°C (except when 37°C is specified) and quenched with 400 μl of 20 mM EDTA (pH 6.0 measured in D_2O), and then 11 μl of 5 M NaCl was added for analysis. For real-time monitoring of enzyme activity, 36 ng (0.8 μM) ITPK1 was used. Reactions (600 μl) were incubated at 25°C in an NMR instrument and measured consecutively with 85 sec spectra. Samples were measured as previously described (Harmel et al., 2019) on Bruker AV-III spectrometers (Bruker Biospin, Rheinstetten, Germany) using cryogenically cooled 5-mm TCI-triple resonance probe equipped with one-axis self-shielded gradients and operating at 600 MHz for proton nuclei, 151 MHz for carbon nuclei, and 244 MHz for P nuclei. The software to control the spectrometer was TopSpin 3.5 pl 6. Temperature was calibrated using d_4-methanol and the formula of Findeisen et al. (2007).

InsPs extraction from seedlings and HPLC analyses

Seedlings were grown vertically on half-strength Murashige and Skoog medium supplemented with 1% sucrose and 7 g/l Phytagel (P8169, Sigma) (pH 5.7) for 12 days (8 h light at 22°C, 16 h darkness at 20°C). Ten to 20 seedlings were transferred to 3 ml half-strength Murashige and Skoog liquid medium without sucrose and with 625 μM P_i (+P) or 5 μM P_i (−P). Seedlings were labeled by adding 30 μCi ml^{-1} of [^{3}H]*myo*-inositol (30–80 Ci $mmol^{-1}$ and 1 mCi ml^{-1}; American Radiolabeled Chemicals) and further cultivated for 5 days. For P_i resupply, 620 μM KH_2PO_4 was added to the medium and the plants were grown for another 6 h before harvest. Afterward, seedlings were washed two times with ultrapure water and frozen in liquid N_2 and the InsPs were extracted as described previously (Azevedo and Saiardi, 2006) and resolved exactly as described in Gaugler et al. (2020).

Statistical analysis

To analyze the significant differences among multiple groups, one-way analysis of variance followed by Tukey's test at $P < 0.05$ was adopted. The statistical significance between two groups was assessed by two-tailed Student's *t*-test. All statistical tests were performed using SigmaPlot 11.0 software.

SUPPLEMENTAL INFORMATION

Supplemental information is available at *Molecular Plant Online*.

FUNDING

This work was funded by grants from the Deutsche Forschungsgemeinschaft (HE 8362/1-1, DFG Eigene Stelle, to R.F.H.G.; SCHA 1274/4-1, SCHA 1274/5-1, Research Training Group GRK 2064 and Germany's Excellence Strategy, EXC-2070-390732324, PhenoRob to G.S.; JE 572/4-1 and Germany's Excellence Strategy, CIBSS–EXC-2189–Project ID 390939984 to H.J.J; and LA 4541/1-1 postdoctoral research

fellowship to D.L.), grants from the Medical Research Council (MRC award MR/T028904/1 to A.S.), and a DBT-IISc Program to D.L.

AUTHOR CONTRIBUTIONS

G.S. and R.F.H.G. conceived the study. D.L., R.K.H., M.F., G.S., and R.F.H.G. designed experiments. E.R., D.L., R.K.H., P.G., V.P., M.F., N.P.L., L.K., R.S., and R.F.H.G. performed experiments. D.Q. performed CE-ESI-MS/MS analysis and isomer identification. M.-R.H. performed UPLC analysis of ATP and ADP. A.S., D.F., H.J.J., G.S., and R.F.H.G. supervised the experimental work. R.F.H.G. and G.S. wrote the manuscript with input from all authors.

ACKNOWLEDGMENTS

We thank Annett Bieber, Jacqueline Fuge, Nicole Schäfer, Yudelsy A. Tandron Moya (Leibniz Institute of Plant Genetics and Crop Plant Research, IPK-Gatersleben), and Li Schlüter (Department of Plant Nutrition, Institute of Crop Science and Resource Conservation) for excellent technical assistance, and Nicolaus von Wirén (IPK-Gatersleben) for critically reading the article. We thank Michael Hothorn (University of Geneva) and Saikat Bhattacharjee (RCB, India) for providing seeds of published mutants. No conflicts of interest declared.

Received: April 6, 2021
Revised: June 28, 2021
Accepted: July 13, 2021
Published: July 14, 2021

REFERENCES

Adepoju, O., Williams, S.P., Craige, B., Cridland, C.A., Sharpe, A.K., Brown, A.M., Land, E., Perera, I.Y., Mena, D., Sobrado, P., et al. (2019). Inositol trisphosphate kinase and diphosphoinositol pentakisphosphate kinase enzymes constitute the inositol pyrophosphate synthesis pathway in plants. bioRxiv, 724914.

An, Y., Jessen, H.J., Wang, H., Shears, S.B., and Kireev, D. (2019). Dynamics of substrate processing by PPIP5K2, a versatile catalytic machine. Structure **27**:1022–1028.e2.

Aung, K., Lin, S.I., Wu, C.C., Huang, Y.T., Su, C.L., and Chiou, T.J. (2006). pho2, a phosphate overaccumulator, is caused by a nonsense mutation in a MicroRNA399 target gene. Plant Physiol. **141**:1000–1011.

Azevedo, C., and Saiardi, A. (2006). Extraction and analysis of soluble inositol polyphosphates from yeast. Nat. Protoc. **1**:2416–2422.

Azevedo, C., and Saiardi, A. (2017). Eukaryotic phosphate homeostasis: the inositol pyrophosphate perspective. Trends Biochem. Sci. **42**:219–231.

Bari, R., Pant, B.D., Stitt, M., and Scheible, W.R. (2006). PHO2, microRNA399, and PHR1 define a phosphate-signaling pathway in plants. Plant Physiol. **141**:988–999.

Bustos, R., Castrillo, G., Linhares, F., Puga, M.I., Rubio, V., Perez-Perez, J., Solano, R., Leyva, A., and Paz-Ares, J. (2010). A central regulatory system largely controls transcriptional activation and repression responses to phosphate starvation in Arabidopsis. PLoS Genet. **6**:e1001102.

Caddick, S.E.K., Harrison, C.J., Stavridou, I., Mitchell, J.L., Hemmings, A.M., and Brearley, C.A. (2008). A Solanum tuberosum inositol phosphate kinase (StITPK1) displaying inositol phosphate-inositol phosphate and inositol phosphate-ADP phosphotransferase activities. Febs Lett. **582**:1731–1737.

Capolicchio, S., Thakor, D.T., Linden, A., and Jessen, H.J. (2013). Synthesis of unsymmetric diphospho-inositol polyphosphates. Angew. Chem. Int. Ed. Engl. **52**:6912–6916.

Delhaize, E., and Randall, P.J. (1995). Characterization of a phosphate-accumulator mutant of Arabidopsis-thaliana. Plant Physiol. **107**:207–213.

Desai, M., Rangarajan, P., Donahue, J.L., Williams, S.P., Land, E.S., Mandal, M.K., Phillippy, B.Q., Perera, I.Y., Raboy, V., and Gillaspy, G.E. (2014). Two inositol hexakisphosphate kinases drive inositol pyrophosphate synthesis in plants. Plant J. **80**:642–653.

Desfougeres, Y., Wilson, M.S.C., Laha, D., Miller, G.J., and Saiardi, A. (2019). ITPK1 mediates the lipid-independent synthesis of inositol phosphates controlled by metabolism. Proc. Natl. Acad. Sci. U S A **116**:24551–24561.

Dong, J., Ma, G., Sui, L., Wei, M., Satheesh, V., Zhang, R., Ge, S., Li, J., Zhang, T.E., Wittwer, C., et al. (2019). Inositol pyrophosphate InsP8 acts as an intracellular phosphate signal in Arabidopsis. Mol. Plant **12**:1463–1473.

Draskovic, P., Saiardi, A., Bhandari, R., Burton, A., Ilc, G., Kovacevic, M., Snyder, S.H., and Podobnik, M. (2008). Inositol hexakisphosphate kinase products contain diphosphate and triphosphate groups. Chem. Biol. **15**:274–286.

Duan, K., Yi, K.K., Dang, L., Huang, H.J., Wu, W., and Wu, P. (2008). Characterization of a sub-family of Arabidopsis genes with the SPX domain reveals their diverse functions in plant tolerance to phosphorus starvation. Plant J. **54**:965–975.

Findeisen, M., Brand, T., and Berger, S. (2007). A 1H-NMR thermometer suitable for cryoprobes. Magn. Reson. Chem. **45**:175–178.

Gaugler, P., Gaugler, V., Kamleitner, M., and Schaaf, G. (2020). Extraction and quantification of soluble, radiolabeled inositol polyphosphates from different plant species using SAX-HPLC. J. Vis. Exp. https://doi.org/10.3791/61495.

Gerasimaite, R., Pavlovic, I., Capolicchio, S., Hofer, A., Schmidt, A., Jessen, H.J., and Mayer, A. (2017). Inositol pyrophosphate specificity of the SPX-dependent polyphosphate polymerase VTC. Acs Chem. Biol. **12**:648–653.

Harmel, R.K., Puschmann, R., Nguyen Trung, M., Saiardi, A., Schmieder, P., and Fiedler, D. (2019). Harnessing (13)C-labeled myo-inositol to interrogate inositol phosphate messengers by NMR. Chem. Sci. **10**:5267–5274.

Kuo, H.F., Chang, T.Y., Chiang, S.F., Wang, W.D., Charng, Y.Y., and Chiou, T.J. (2014). Arabidopsis inositol pentakisphosphate 2-kinase, AtIPK1, is required for growth and modulates phosphate homeostasis at the transcriptional level. Plant J. **80**:503–515.

Kuo, H.F., Hsu, Y.Y., Lin, W.C., Chen, K.Y., Munnik, T., Brearley, C.A., and Chiou, T.J. (2018). Arabidopsis inositol phosphate kinases IPK1 and ITPK1 constitute a metabolic pathway in maintaining phosphate homeostasis. Plant J. **95**:613–630.

Laha, D., Johnen, P., Azevedo, C., Dynowski, M., Weiss, M., Capolicchio, S., Mao, H., Iven, T., Steenbergen, M., Freyer, M., et al. (2015). VIH2 regulates the synthesis of inositol pyrophosphate InsP8 and jasmonate-dependent defenses in Arabidopsis. Plant Cell **27**:1082–1097.

Laha, D., Parvin, N., Dynowski, M., Johnen, P., Mao, H., Bitters, S.T., Zheng, N., and Schaaf, G. (2016). Inositol polyphosphate binding specificity of the jasmonate receptor complex. Plant Physiol. **171**:2364–2370.

Laha, D., Parvin, N., Hofer, A., Giehl, R.F.H., Fernandez-Rebollo, N., von Wiren, N., Saiardi, A., Jessen, H.J., and Schaaf, G. (2019). Arabidopsis ITPK1 and ITPK2 have an evolutionarily conserved phytic acid kinase activity. Acs Chem. Biol. **14**:2127–2133.

Laha, N.P., Dhir, Y.W., Giehl, R.F.H., Schaefer, E.M., Gaugler, P., Shishavan, Z.H., Gulabani, H., Mao, H., Zheng, N., von Wiren, N., et al. (2020). ITPK1-Dependent inositol polyphosphates regulate auxin responses in *Arabidopsis thaliana*. bioRxiv, 2020.2004.2023.058487.

Please cite this article in press as: Riemer et al., ITPK1 is an $InsP_6$/ADP phosphotransferase that controls phosphate signaling in *Arabidopsis*, Molecular Plant (2021), https://doi.org/10.1016/j.molp.2021.07.011

Laussmann, T., Reddy, K.M., Reddy, K.K., Falck, J.R., and Vogel, G. (1997). Diphospho-myo-inositol phosphates from Dictyostelium identified as D-6-diphospho-myo-inositol pentakisphosphate and D-5,6-bisdiphospho-myo-inositol tetrakisphosphate. Biochem. J. **322**:31–33.

Lin, S.I., Chiang, S.F., Lin, W.Y., Chen, J.W., Tseng, C.Y., Wu, P.C., and Chiou, T.J. (2008). Regulatory network of microRNA399 and PHO2 by systemic signaling. Plant Physiol. **147**:732–746.

Liu, F., Wang, Z.Y., Ren, H.Y., Shen, C.J., Li, Y., Ling, H.Q., Wu, C.Y., Lian, X.M., and Wu, P. (2010). OsSPX1 suppresses the function of OsPHR2 in the regulation of expression of OsPT2 and phosphate homeostasis in shoots of rice. Plant J. **62**:508–517.

Losito, O., Szijgyarto, Z., Resnick, A.C., and Saiardi, A. (2009). Inositol pyrophosphates and their unique metabolic complexity: analysis by gel electrophoresis. PLoS One **4**:e5580.

Luo, H.B.R., Huang, Y.E., Chen, J.M.C., Saiardi, A., Iijima, M., Ye, K.Q., Huang, Y.F., Nagata, E., Devreotes, P., and Snyder, S.H. (2003). Inositol pyrophosphates mediate chemotaxis in Dictyostelium via pleckstrin homology domain-PtdIns (3,4,5)P3 interactions. Cell **114**:559–572.

Lv, Q.D., Zhong, Y.J., Wang, Y.G., Zhang, L., Shi, J., Wu, Z.C., Liu, Y., Mao, C.Z., Yi, K.K., and Wu, P. (2014). SPX4 negatively regulates phosphate signaling and homeostasis through its interaction with PHR2 in rice. Plant Cell **26**:1586–1597.

Miller, G.J., Wilson, M.P., Majerus, P.W., and Hurley, J.H. (2005). Specificity determinants in inositol polyphosphate synthesis: crystal structure of inositol 1,3,4-trisphosphate 5/6-kinase. Mol. Cell **18**:201–212.

Mulugu, S., Bai, W.L., Fridy, P.C., Bastidas, R.J., Otto, J.C., Dollins, D.E., Haystead, T.A., Ribeiro, A.A., and York, J.D. (2007). A conserved family of enzymes that phosphorylate inositol hexakisphosphate. Science **316**:106–109.

Nagy, R., Grob, H., Weder, B., Green, P., Klein, M., Frelet-Barrand, A., Schjoerring, J.K., Brearley, C., and Martinoia, E. (2009). The Arabidopsis ATP-binding cassette protein AtMRP5/AtABCC5 is a high affinity inositol hexakisphosphate transporter involved in guard cell signaling and phytate storage. J. Biol. Chem. **284**:33614–33622.

Pfaffl, M.W. (2001). A new mathematical model for relative quantification in real-time RT-PCR. Nucleic Acids Res. **29**:e45.

Puga, M.I., Mateos, I., Charukesi, R., Wang, Z., Franco-Zorrilla, J.M., de Lorenzo, L., Irigoye, M.L., Masiero, S., Bustos, R., Rodriguez, J., et al. (2014). SPX1 is a phosphate-dependent inhibitor of PHOSPHATE STARVATION RESPONSE 1 in Arabidopsis. Proc. Natl. Acad. Sci. U S A **111**:14947–14952.

Puschmann, R., Harmel, R.K., and Fiedler, D. (2019). Scalable chemoenzymatic synthesis of inositol pyrophosphates. Biochemistry **58**:3927–3932.

Qi, W.J., Manfield, I.W., Muench, S.P., and Baker, A. (2017). AtSPX1 affects the AtPHR1-DNA-binding equilibrium by binding monomeric AtPHR1 in solution. Biochem. J. **474**:3675–3687.

Qiu, D., Wilson, M.S., Eisenbeis, V.B., Harmel, R.K., Riemer, E., Haas, T.M., Wittwer, C., Jork, N., Gu, C., Shears, S.B., et al. (2020). Analysis of inositol phosphate metabolism by capillary electrophoresis electrospray ionization mass spectrometry. Nat. Commun. **11**:6035.

Reski, R., and Abel, W.O. (1985). Induction of budding on chloronemata and caulonemata of the moss, Physcomitrella patens, using isopentenyladenine. Planta **165**:354–358.

Ried, M.K., Wild, R., Zhu, J., Pipercevic, J., Sturm, K., Broger, L., Harmel, R.K., Abriata, L.A., Hothorn, L.A., Fiedler, D., et al. (2021). Inositol pyrophosphates promote the interaction of SPX domains with the coiled-coil motif of PHR transcription factors to regulate plant phosphate homeostasis. Nat. Commun. **12**:384.

Rubio, V., Linhares, F., Solano, R., Martin, A.C., Iglesias, J., Leyva, A., and Paz-Ares, J. (2001). A conserved MYB transcription factor involved in phosphate starvation signaling both in vascular plants and in unicellular algae. Gene Dev. **15**:2122–2133.

Rus, A., Baxter, I., Muthukumar, B., Gustin, J., Lahner, B., Yakubova, E., and Salt, D.E. (2006). Natural variants of AtHKT1 enhance Na+ accumulation in two wild Populations of Arabidopsis. PLoS Genet. **2**:1964–1973.

Saiardi, A., Erdjument-Bromage, H., Snowman, A.M., Tempst, P., and Snyder, S.H. (1999). Synthesis of diphosphoinositol pentakisphosphate by a newly identified family of higher inositol polyphosphate kinases. Curr. Biol. **9**:1323–1326.

Schaaf, G., Betts, L., Garrett, T.A., Raetz, C.R., and Bankaitis, V.A. (2006). Crystallization and preliminary X-ray diffraction analysis of phospholipid-bound Sfh1p, a member of the Saccharomyces cerevisiae Sec14p-like phosphatidylinositol transfer protein family. Acta Crystallogr. F Struct. Biol. Cryst. Commun. **62**:1156–1160.

Shears, S.B. (2018). Intimate connections: inositol pyrophosphates at the interface of metabolic regulation and cell signaling. J. Cell Physiol. **233**:1897–1912.

Stevenson-Paulik, J., Bastidas, R.J., Chiou, S.T., Frye, R.A., and York, J.D. (2005). Generation of phytate-free seeds in Arabidopsis through disruption of inositol polyphosphate kinases. Proc. Natl. Acad. Sci. U S A **102**:12612–12617.

Voglmaier, S.M., Bembenek, M.E., Kaplin, A.I., Dorman, G., Olszewski, J.D., Prestwich, G.D., and Snyder, S.H. (1996). Purified inositol hexakisphosphate kinase is an ATP synthase: diphosphoinositol pentakisphosphate as a high-energy phosphate donor. Proc. Natl. Acad. Sci. U S A **93**:4305–4310.

Wang, H.C., Godage, H.Y., Riley, A.M., Weaver, J.D., Shears, S.B., and Potter, B.V.L. (2014a). Synthetic inositol phosphate analogs reveal that PPIP5K2 has a surface-mounted substrate capture site that is a target for drug discovery. Chem. Biol. **21**:689–699.

Wang, Z.Y., Ruan, W.Y., Shi, J., Zhang, L., Xiang, D., Yang, C., Li, C.Y., Wu, Z.C., Liu, Y., Yu, Y.A., et al. (2014b). Rice SPX1 and SPX2 inhibit phosphate starvation responses through interacting with PHR2 in a phosphate-dependent manner. Proc. Natl. Acad. Sci. U S A **111**:14953–14958.

Whitfield, H., White, G., Sprigg, C., Riley, A.M., Potter, B.V.L., Hemmings, A.M., and Brearley, C.A. (2020). An ATP-responsive metabolic cassette comprised of inositol tris/tetrakisphosphate kinase 1 (ITPK1) and inositol pentakisphosphate 2-kinase (IPK1) buffers diphosphoinositol phosphate levels. Biochem. J. **477**:2621–2638.

Wild, R., Gerasimaite, R., Jung, J.Y., Truffault, V., Pavlovic, I., Schmidt, A., Saiardi, A., Jessen, H.J., Poirier, Y., Hothorn, M., et al. (2016). Control of eukaryotic phosphate homeostasis by inositol polyphosphate sensor domains. Science **352**:986–990.

Wilson, M.S., and Saiardi, A. (2018). Inositol phosphates purification using titanium dioxide beads. Bio Protoc. **8**:e2959.

Wilson, M.S.C., Bulley, S.J., Pisani, F., Irvine, R.F., and Saiardi, A. (2015). A novel method for the purification of inositol phosphates from biological samples reveals that no phytate is present in human plasma or urine. Open Biol. **5**:150014.

Wilson, M.S.C., Livermore, T.M., and Saiardi, A. (2013). Inositol pyrophosphates: between signalling and metabolism. Biochem. J. **452**:369–379.

Wundenberg, T., Grabinski, N., Lin, H.Y., and Mayr, G.W. (2014). Discovery of InsP(6)-kinases as InsP(6)-dephosphorylating enzymes provides a new mechanism of cytosolic InsP(6) degradation driven by the cellular ATP/ADP ratio. Biochem. J. **462**:173–184.

Zhong, Y., Wang, Y., Guo, J., Zhu, X., Shi, J., He, Q., Liu, Y., Wu, Y., Zhang, L., Lv, Q., et al. (2018). Rice SPX6 negatively regulates the phosphate starvation response through suppression of the transcription factor PHR2. New Phytol. **219**:135–148.

Zhu, J., Lau, K., Puschmann, R., Harmel, R.K., Zhang, Y., Pries, V., Gaugler, P., Broger, L., Dutta, A.K., Jessen, H.J., et al. (2019). Two bifunctional inositol pyrophosphate kinases/phosphatases control plant phosphate homeostasis. eLife **8**:e43582.

Molecular Plant, Volume *14*

Supplemental information

ITPK1 is an $InsP_6$/ADP phosphotransferase that controls phosphate signaling in *Arabidopsis*

Esther Riemer, Danye Qiu, Debabrata Laha, Robert K. Harmel, Philipp Gaugler, Verena Gaugler, Michael Frei, Mohammad-Reza Hajirezaei, Nargis Parvin Laha, Lukas Krusenbaum, Robin Schneider, Adolfo Saiardi, Dorothea Fiedler, Henning J. Jessen, Gabriel Schaaf, and Ricardo F.H. Giehl

Suppl. Table 1. Expression of P_i starvation-induced genes in response to changes in P_i availability. Wild-type plants (Col-0) were cultivated in hydroponics under sufficient P_i (+P), deficient P_i for 7 days (-P) or resupplied with P_i for 6 h. Values represent expression levels normalized to +P. Shown are means ± SE (*n* = 3 biological replicates).

Gene	**+P**	**-P**	**Pi RS 6h**
SPX1	1.0 ± 0.17	267 ± 10.53	6.93 ± 1.59
IPS1	1.0 ± 0.27	1601 ± 154	90 ± 13.8
PHR1	1.0 ± 0.06	1.04 ± 0.05	0.86 ± 0.03
PHT1;1	1.0 ± 0.22	16.4 ± 1.93	2.42 ± 0.52
PHT1;2	1.0 ± 0.19	126.67 ± 10.88	10.14 ± 0.79
PHT1;8	1.0 ± 0.23	50.39 ± 5.75	8.11 ± 0.57
PHT1;9	1.0 ± 0.07	27.06 ± 4.21	3.08 ± 0.58

Suppl. Table 2. List of primers used in this study.

Primers used for qPCR analysis		
AGI ID	**Gene name**	**Primer sequence**
AT2G36170	*UBQ2*	F: 5'-CCAAGATCCAGGACAAAGAAGGA-3' R: 5'-TGGAGACGAGCATAACACTTG-3'
AT5G43350	*PHT1;1*	F: 5'-AGGCGATCACGTTGCTTACA-3' R: 5'- TCTCTGGAGAGTTGAGGAGAGAC-3'
AT5G43370	*PHT1;2*	F: 5'-CCATTAGCGCACAACGGAAAG-3' R: 5'-GAAACCCATACCGGCGATGA-3'
AT5G43360	*PHT1;3*	F: 5'-GCTTTCATCGCGGCAGTGTT-3' R: 5'-TGAGGAGGCGTTGATAGAAACC-3'
AT2G38940	*PHT1;4*	F: 5'-AGCCTTTGTCTCTGCGGTTT-3' R: 5'-CGTGGATCCCAAGGCATCAT-3'
AT1G20860	*PHT1;8*	F: 5'-AGAGAAGTGGCGGTGGTTTG-3' R: 5'-TCTTGCGGTTTCAGGCATCA-3'
AT1G76430	*PHT1;9*	F: 5'-TTCGGAGAAGACGAACGTGG-3' R: 5'-GTATCTGGCGGTTTCAGGCA-3'
AT3G23430	*PHO1*	F: 5'-GACTTACAGCTCGTTGAATATGATAGC-3' R: 5'-CGATCTCTTTACGACTTTGAGATACG-3'
AT4G28610	*PHR1*	F: 5'-TGTGGAATTGCGACCTGTTA-3' R: 5'-GCTCTTTCACTACCGCCAAG-3'
AT5G20150	*SPX1*	F: 5'-GTTGATTTCCATGGAGAAATGG-3' R: 5'-GGTAAACGCATGAGATCACCAG-3'
AT3G09922	*IPS1*	F: 5'-TCCCTCTAGAAATTGGGCAAC-3' R: 5'-GGGAGTGGGTACAACCCAAA-3'
AT2G33770	*PHO2*	F: 5'-TTGCACCATGTGAAATTTGG-3' R: 5'-AGACCCGTTTCCTGATGGTT-3'
AT5G16760	*ITPK1*	F: 5'-ATTGGGACGTCGAAAGGGTC-3' R: 5'-CTCAGTCAACACAGGCTCGT-3'
Primers used for genotyping in F1, F2 and F3		
itpk1_LP	5'-ACCAATATTCGATTCCACACG-3'	
itpk1_RP	5'-CCATGTCCCAGAAGAACTCAG-3'	
itpk2-2_LP	5'- TCGCTTGTACTTTTCAAGTTGC-3'	

itpk2-2_RP	5'- TAAGGACAAAAACATGGCAGG-3'
SAIL_LB3	5'-TAGCATCTGAATTTCATAACCAATCTCGATACAC-3'
phr1_LP	5'-GAGAGACCTCACACGCACTTC-3'
phr1_RP	5'-CTTTCTGGCGAACCTGTAGTG-3'
phl1_LP	5'-GTGGAGACGTTTCTGCACTTC-3'
phl1_RP	5'-TCCCACAATCCAAATTCAGAG-3'
LBb1.3	5'-ATTTTGCCGATTTCGGAAC-3'
vih2-4_GK_LP	5'-AACAACAGCAATGACACAACG-3'
vih2-4_GK_RP	5'-CATTCCCATCTTTTGGACAAC-3'
GABI_LB1	5'-ATAATAACGCTGCGGACATCTACATTTT-3'

Suppl. Table 3. Mass spectrometer parameters used for the analysis of inositol (pyro)phosphates.

Compound	MRM transitions	Type of transition	Collision Energy (V)	Cell Acc (V)
$InsP_8$	408.9 → 359.6[a] 408.9 → 78.9	$[M-2H]^{2-} \rightarrow [M-2H-H_3PO_4]^{2-}$ $[M-2H]^{2-} \rightarrow [PO_3]^-$	10 42	1 4
$[^{13}C_6]InsP_8$	411.9 → 362.6[a] 411.9 → 78.9	$[M-2H]^{2-} \rightarrow [M-2H-H_3PO_4]^{2-}$ $[M-2H]^{2-} \rightarrow [PO_3]^-$	10 42	1 4
$InsP_7$	368.9 → 319.6[a] 368.9 → 78.9	$[M-2H]^{2-} \rightarrow [M-2H-H_3PO_4]^{2-}$ $[M-2H]^{2-} \rightarrow [PO_3]^-$	10 38	3 3
$[^{13}C_6]InsP_7$	371.9 → 322.6[a] 371.9 → 78.9	$[M-2H]^{2-} \rightarrow [M-2H-H_3PO_4]^{2-}$ $[M-2H]^{2-} \rightarrow [PO_3]^-$	10 38	3 3
$InsP_6$	328.9 → 78.9[a] 328.9 → 481	$[M-2H]^{2-} \rightarrow [PO_3]^-$ $[M-2H]^{2-} \rightarrow [M-H-HPO_3-H_3PO_4]^-$	46 10	1 3
$[^{13}C_6]InsP_6$	331.9 → 78.9[a] 331.9 → 487	$[M-2H]^{2-} \rightarrow [PO_3]^-$ $[M-2H]^{2-} \rightarrow [M-H-HPO_3-H_3PO_4]^-$	46 10	1 3
$InsP_5$	288.9 → 498.7[a] 288.9 → 78.9	$[M-2H]^{2-} \rightarrow [M-H-HPO_3]^-$ $[M-2H]^{2-} \rightarrow [PO_3]^-$	10 14	1 1
$[^{13}C_6]InsP_5$	291.0 → 504.7[a] 291.0 → 78.9	$[M-2H]^{2-} \rightarrow [M-H-HPO_3]^-$ $[M-2H]^{2-} \rightarrow [PO_3]^-$	10 14	1 1
$InsP_4$	249.0 → 418.6[a] 249.0 → 320.6	$[M-2H]^{2-} \rightarrow [M-H-HPO_3]^-$ $[M-2H]^{2-} \rightarrow [M-H-HPO_3-H_3PO_4]^-$	10 14	1 1
$InsP_3$	419.0 → 320.6[a] 419.0 → 78.9	$[M-H]^- \rightarrow [M-H-H_3PO_4]^-$ $[M-H]^- \rightarrow [PO_3]^-$	18 50	4 1

[a] MRM transition with the highest response for each compound (used for quantification).

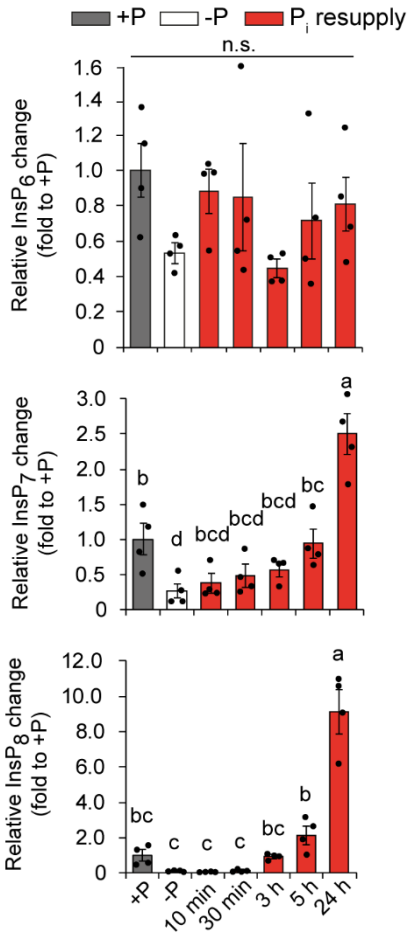

Supplemental Figure 1. InsP$_6$ and InsP$_7$ levels respond strongly to P$_i$ deficiency and P$_i$ resupply in rice plants.

Shown are fold changes of quantified signal intensities of independent PAGE gels. Data are means ± SE (n = 3 gels loaded with independent biological samples). Plants were cultivated in hydroponics under sufficient P$_i$ (+P), deficient P$_i$ (-P) for 10 days, or -P resupplied with P$_i$ for the indicated times. Different letters indicate significant differences according to Tukey's test ($P < 0.05$). n.s., not significant according to one-way ANOVA ($P < 0.05$).

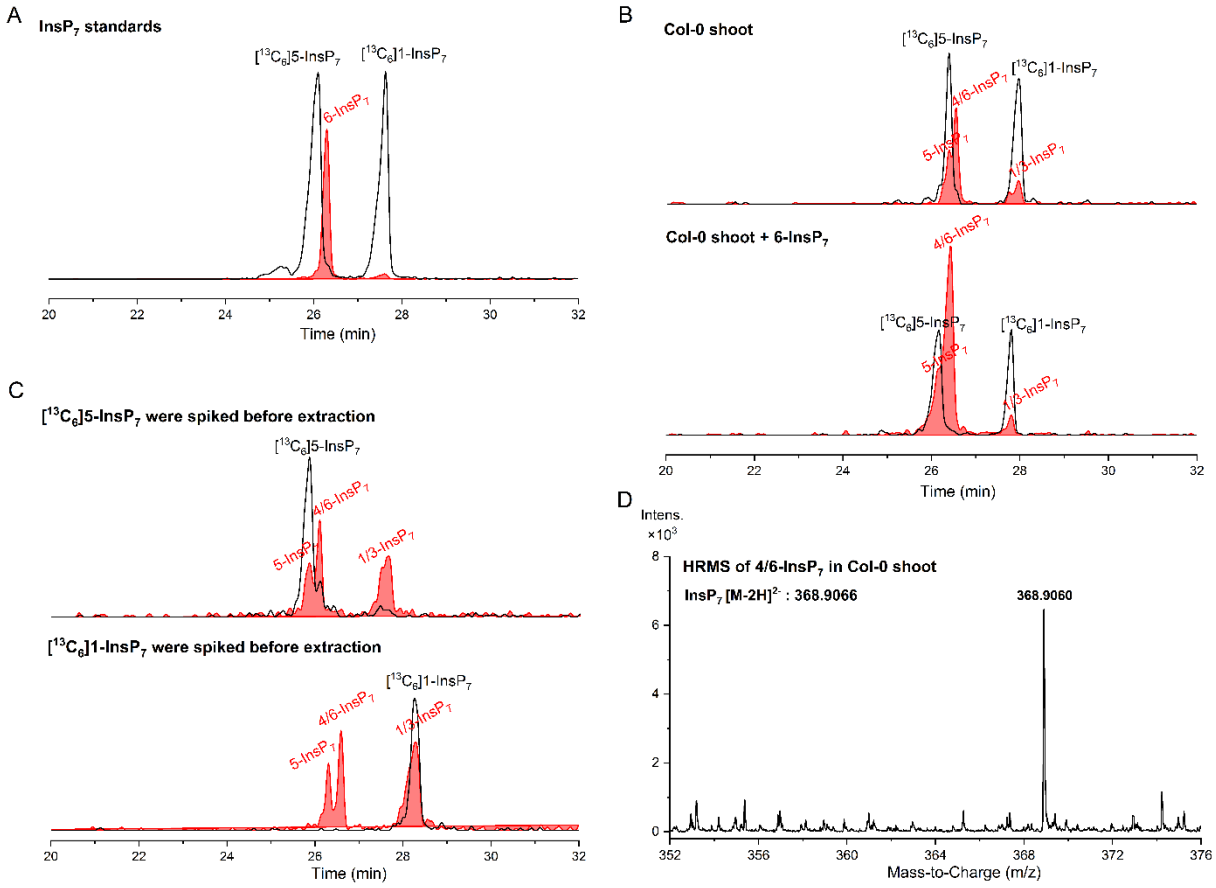

Supplemental Figure 2. Determination of 4/6-InsP$_7$ as a novel PP-InsP found in plants via CE-ESI-qTOF analysis.

(A) 6-InsP$_7$ could be readily distinguished with the aid of isotopic standards [$^{13}C_6$]5-InsP$_7$ and [$^{13}C_6$]1-InsP$_7$ with CE-ESI-MS.

(B) An undefined InsP$_7$ isomer found in *Arabidopsis* (Col-0) showed same migration time as 6-InsP$_7$ standard.

(C) [$^{13}C_6$]5-InsP$_7$ and [$^{13}C_6$]1-InsP$_7$ were spiked before InsP extractions, ruling out the possibility that 4/6-InsP$_7$ were generated during sample preparation.

(D) A representative high-resolution mass spectrum (HRMS) of 4/6-InsP$_7$ in *Arabidopsis*.

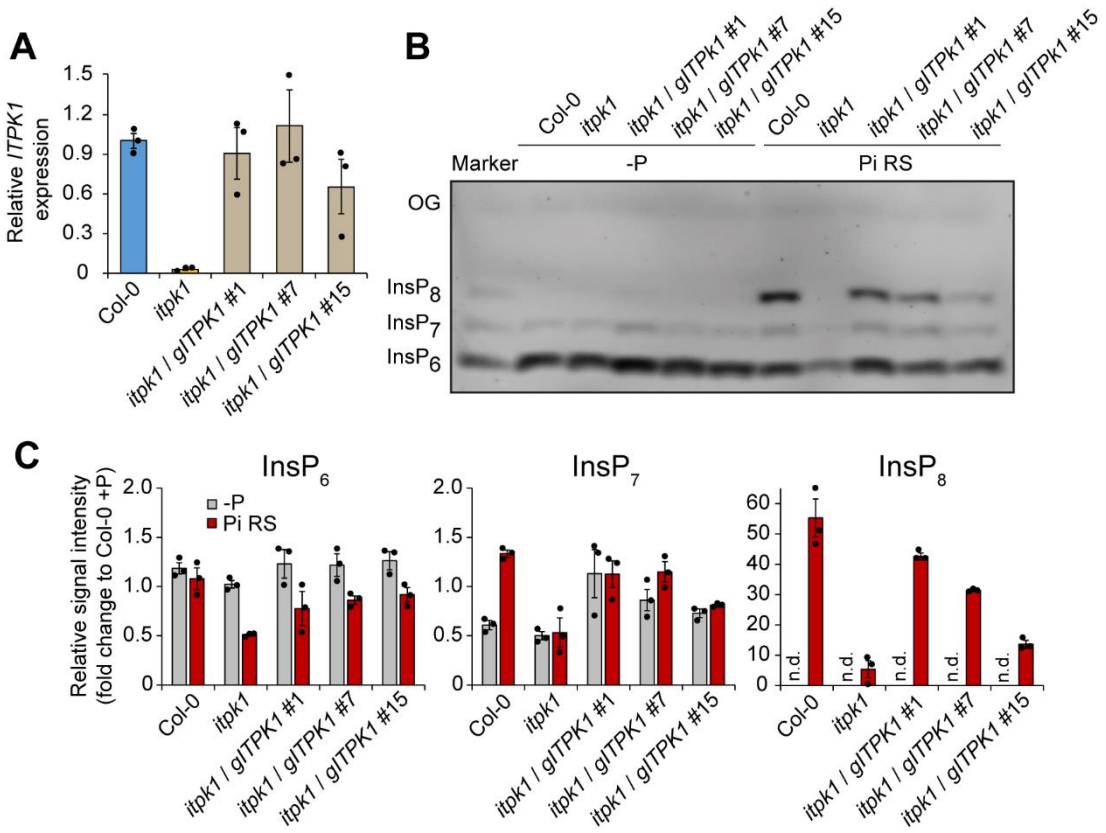

Supplemental Figure 3. Complementation of *itpk1* mutant.

(A) *ITPK1* expression in 3-week-old WT (Col-0), *itpk1* and three independent *itpk1* lines transformed with *ITPK1* genomic DNA. Data represent means ± SD (*n* = 3 biological replicates).

(B and C) PAGE detection **(B)** and fold change of quantified signal intensities **(C)** of inositol (pyro)phosphates in shoots of WT (Col-0), *itpk1* and three independent *itpk1* lines transformed with *ITPK1* genomic DNA. Plants were cultivated in hydroponics under deficient P_i for 7 days (-P) or -P resupplied with P_i for 12 h (Pi RS). Data represent means ± SE of values normalized to Col-0 plants continuously grown under sufficient P_i (*n* = 3 biological replicates). n.d., not detected. OG, orange G.

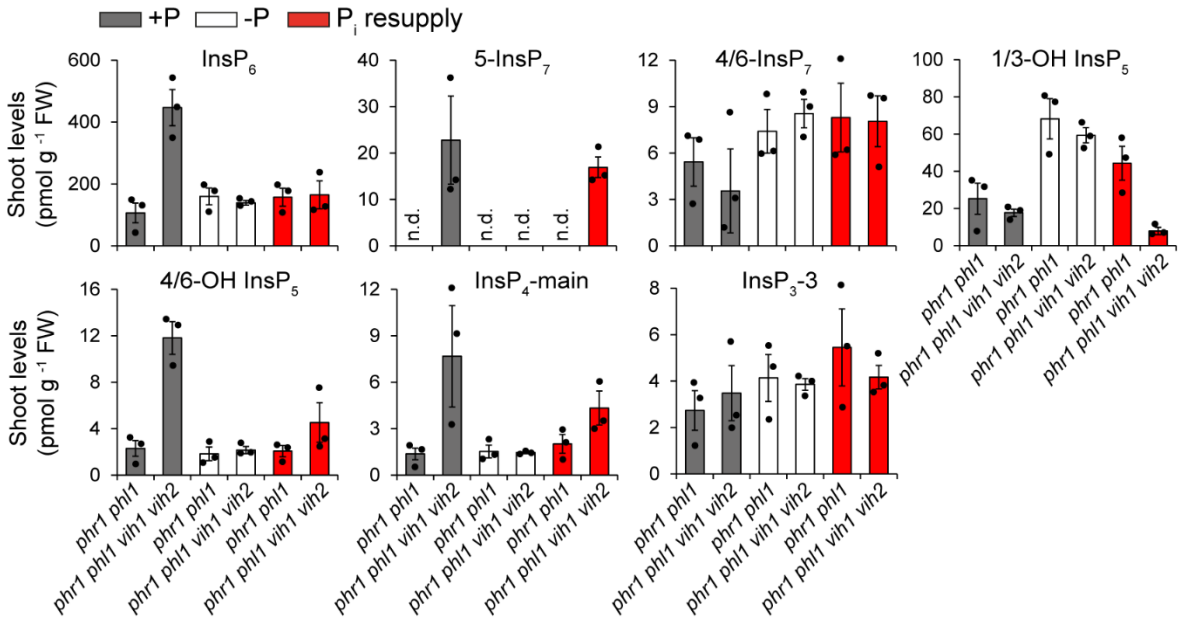

Supplemental Figure 4. VIH1- and VIH2-dependent inositol (pyro)phosphate metabolism.

CE-ESI-MS analysis of *VIH1* and *VIH2* mutations in the *phr1 phl1* background. Plants were cultivated in hydroponics under sufficient P_i (+P), deficient P_i (-P) or -P resupplied with P_i for the indicated times. Data represent means ± SE (*n* = 3 biological replicates). n.d., could not be detected in any of these samples. Note that $InsP_8$, 1/3-$InsP_7$, $InsP_3$-1 and 2-OH $InsP_5$ could not be detected in none of the analyzed samples.

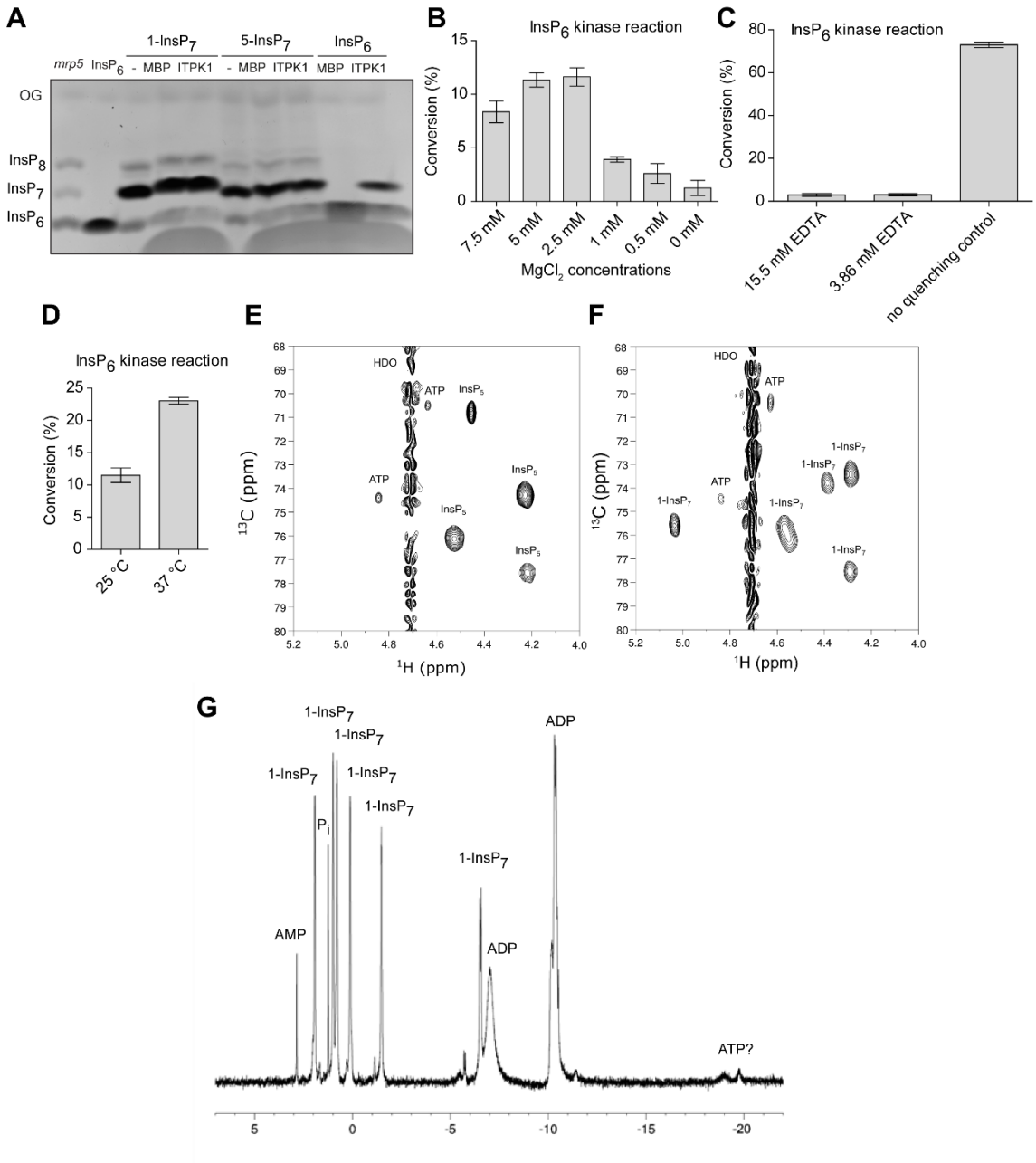

Supplemental Figure 5. Activity of *Arabidopsis* ITPK1 on $InsP_5$ [2-OH] and $InsP_7$ isomers and control experiments for kinase assays.

(A) ITPK1 has no kinase activity on 1-$InsP_7$ and 5-$InsP_7$. $InsP_7$ isomers or $InsP_6$ were incubated with recombinant *Arabidopsis* ITPK1 as indicated in presence of 12.5 mM ATP. Inositol (pyro)phosphates were separated via PAGE and visualized by toluidine blue staining. The identity of bands was determined by migration compared to the substrates in absence of enzyme (-) and TiO_2-purified *mrp5* seed extract. Purified His_8-MBP tag (MBP) served as negative control for ITPK1. OG, orange G.

(B-D) Control experiments for NMR analyses. $InsP_6$ was incubated with recombinant *Arabidopsis* ITPK1 at 25°C in the presence of 2.5 mM ATP. Enzymatic activity was determined after 24 h in the presence of varying EDTA concentrations **(B)**, after 1.5 h at changing Mg^{2+} concentrations **(C)** and temperature **(D)**. The conversion was determined by NMR spectroscopy after quenching with an excess of EDTA.

(E-G) 2D ^{1}H-^{13}C-HMBC spectra. Recombinant *Arabidopsis* ITPK1 was incubated with $InsP_5$ **(E)** or 1-$InsP_7$ **(F)** at 25°C in the presence of an ATP recycling system for 24 h. The reaction mixture was analyzed by HSQC NMR spectroscopy. **(G)** Overview of the reaction shown in **(F)** as analyzed by ^{31}P NMR spectroscopy after 24 h. A small, unidentified signal potentially reflecting ATP is marked with a question mark.

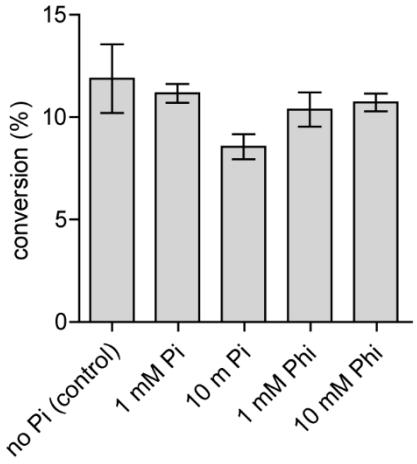

Supplemental Figure 6. Dependency of *Arabidopsis* ITPK1 kinase activity on P_i.
$InsP_6$ was incubated with recombinant *Arabidopsis* ITPK1 at 25°C in the presence of 2.5 mM ATP and the indicated concentrations of P_i or its non-metabolizable analog phosphite (Phi). The conversion was determined by NMR spectroscopy after quenching with an excess of EDTA. The experiment was repeated three times.

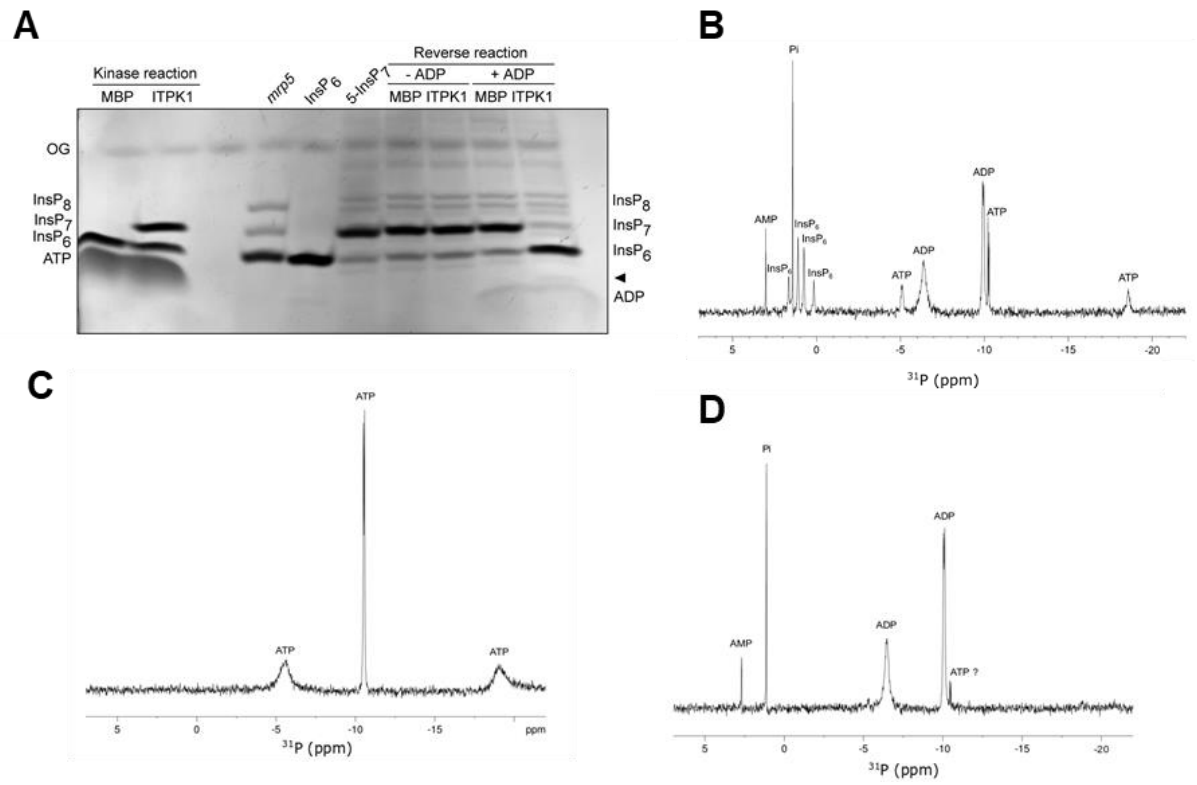

Supplemental Figure 7. Recombinant *Arabidopsis* ITPK1 can dephosphorylate 5-InsP$_7$ in the presence of ADP.

(A) ADP-dependent dephosphorylation of 5-InsP$_7$ by recombinant *Arabidopsis* ITPK1. InsPs were separated via PAGE and visualized by toluidine blue staining. The identity of bands was determined by migration compared to InsP$_6$ and 5-InsP$_7$ standards and TiO_2-purified *mrp5* seed extract. InsP$_6$ kinase reaction served as positive control for the reverse reactions. Purified His$_8$-MBP tag (MBP) served as negative control for ITPK1. Arrowhead indicates the presence of a small ATP band just above ADP. OG, orange G.

(B) ^{31}P NMR spectroscopy analysis of recombinant *Arabidopsis* ITPK1 incubated with [$^{13}C_6$]-labelled 5-InsP$_7$ at 25°C in the presence of ADP. After 24 h the mixture was analyzed by NMR.

(C) ^{31}P NMR analysis of ATP in ATP synthase reaction buffer.

(D) ^{31}P NMR spectroscopy analysis of recombinant *Arabidopsis* ITPK1 incubated with ADP without 5-InsP$_7$ at 25°C and analyzed after 24 h. A small, unidentified signal potentially reflecting ATP is marked with a question mark.

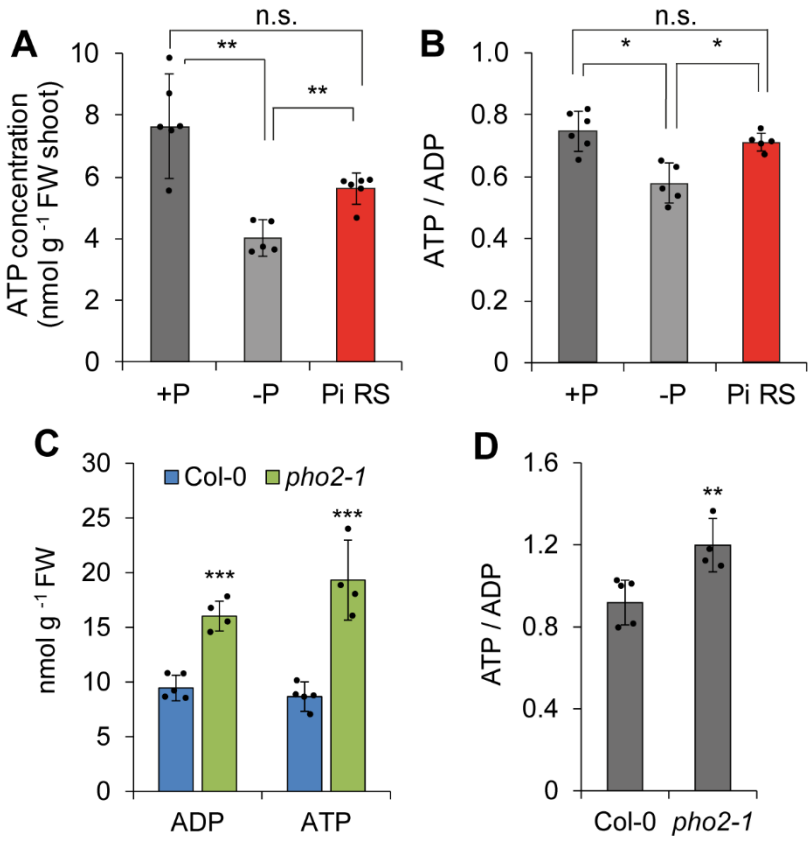

Supplemental Figure 8. Effect of P_i availability and resupply on shoot ATP levels.
(A and B) Concentration of ATP **(A)** and ATP/ADP ratios **(B)** in shoots of Col-0 plants grown in hydroponics with P_i-sufficient solution (+P), exposed to 4 days of P_i starvation (-P) or resupplied with P_i for 12 h (Pi RS). Data represent means ± SD (n = 5-6 biological replicates). n.s., not significant.
(C and D) Concentration of ATP and ADP **(C)** and ATP/ADP ratios **(D)** in shoots of Col-0 and the P-overaccumulating mutant *pho2-1* grown in hydroponics with sufficient P_i. Data represent means ± SD (n = 4-5 biological replicates). *P < 0.05, **P < 0.01 and ***P < 0.001 denote significant difference to wild type (Col-0) according to Student's t-test.

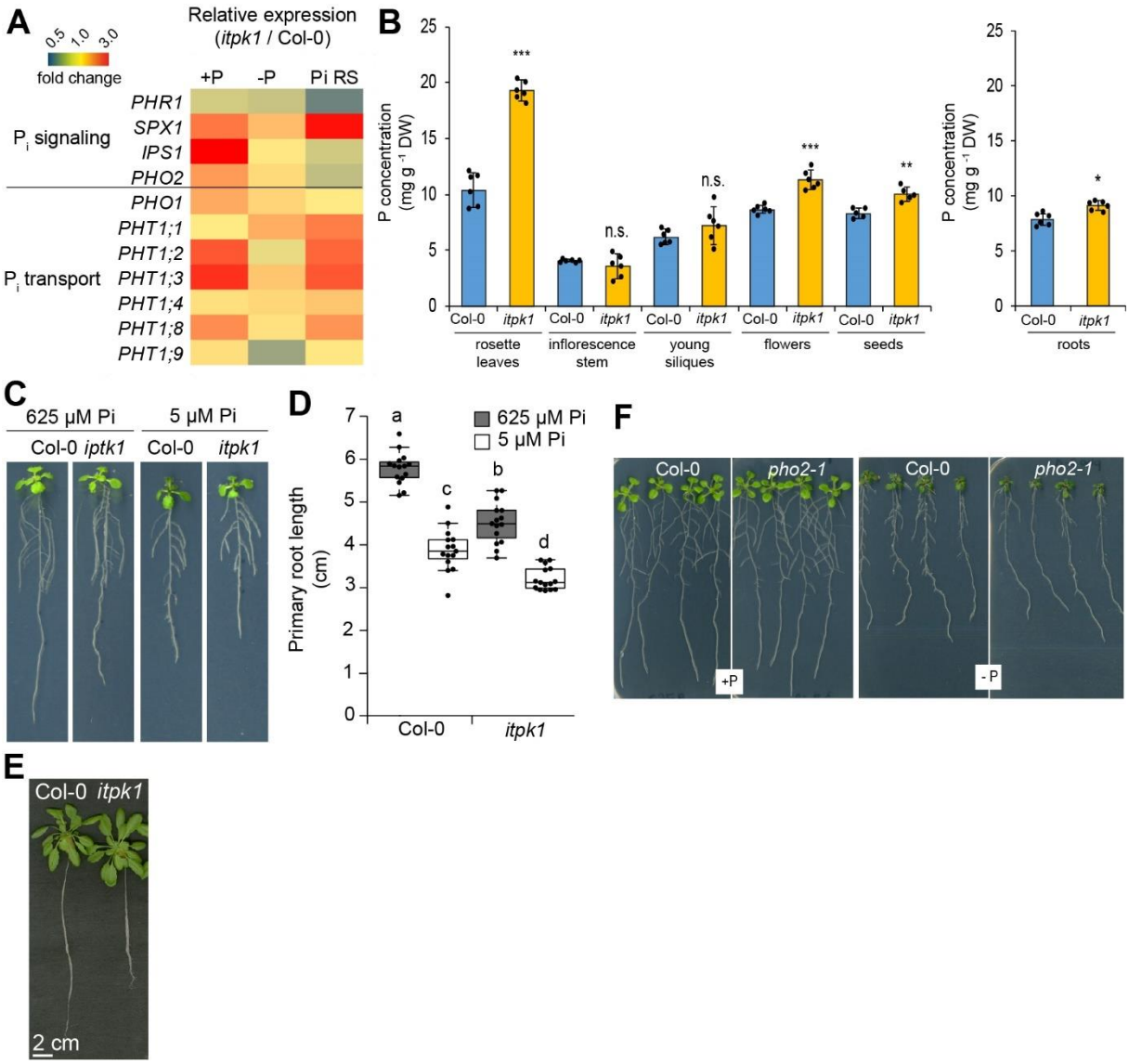

Supplemental Figure 9. ITPK1-dependent P overaccumulation in different plant organs and root phenotypes.

(A) Disruption of *ITPK1* results in mis-regulated expression of P_i starvation-induced genes in roots.

(B) Total P levels in different parts of wild-type (Col-0) and *itpk1* plants. Data represent means ± SD (*n* = samples from 5 independent plants). Samples of above-ground tissues were collected from 5-week-old plants grown on peat-based substrate. Roots were collected from plants grown under sufficient P_i in hydroponics. **P* < 0.05, ***P* < 0.01 and ****P* < 0.001 denote significant difference to wild type (Col-0) according to Student's *t*-test. n.s., not significant. Young siliques = green siliques with a length of 0.8 cm to 1.5 cm.

(C and D) P_i-independent root growth repression in *itpk1* plants. Plant phenotype **(C)** and primary root length **(D)** after 7 days of growth under sufficient (625 µM P_i) or deficient P_i supply (5 µM P_i). Horizontal lines show medians; box limits indicate the 25th and 75th percentiles; whiskers extend to 1.5 times the interquartile range from the 25th and 75th percentiles (*n* = 15 independent plants). Different letters indicate significant differences according to Tukey's test (*P* < 0.05).

(E) Short-root phenotype of 5-week-old *itpk1* plants grown in hydroponics with sufficient P_i. Representative plants are shown.

(F) Phenotype of wild-type (Col-0) and *pho2-1* plants grown in agar plates. Seven-day-old seedlings germinated on half-strength solid Murashige and Skoog agar media containing 625 µM P_i were transferred to +P (625 µM P_i) or -P (5 µM P_i) and grown for additional 7 days until imaging.

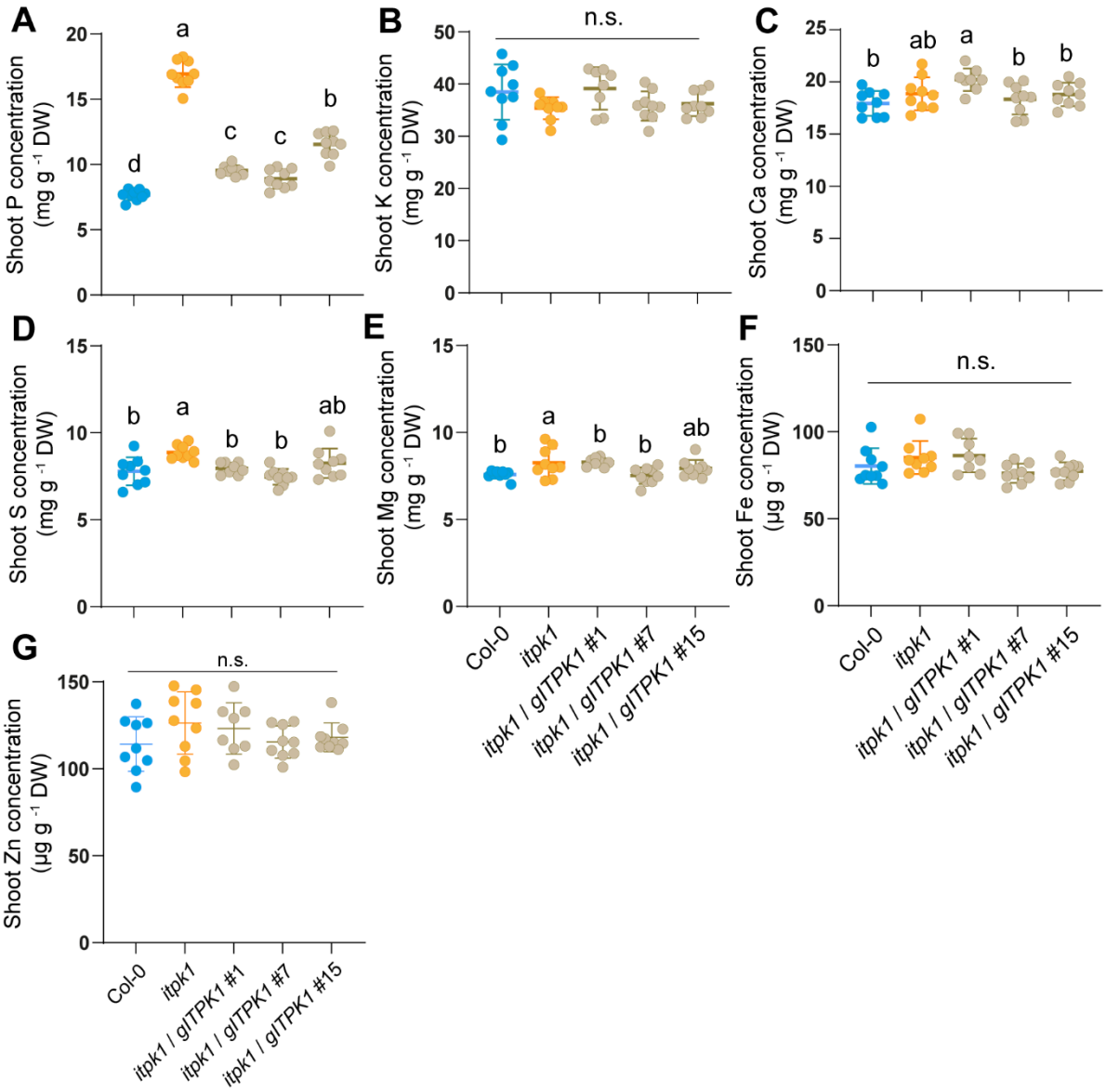

Supplemental Figure 10. The *itpk1* mutant shows a specific overaccumulation of P that can be complemented with genomic *ITPK1*.

Shoot concentrations of the macronutrients phosphorus **(A)**, potassium **(B)**, calcium **(C)**, sulfur **(D)** and magnesium **(E)**, and the micronutrients iron **(F)** and zinc **(G)** of 3-week-old plants grown on peat-based substrate. Graphs depict the means ± SD (n = 8-9 plants) and raw data points. Different letters indicate significant differences according to Tukey's test ($P < 0.05$). n.s., not significant according to one-way ANOVA.

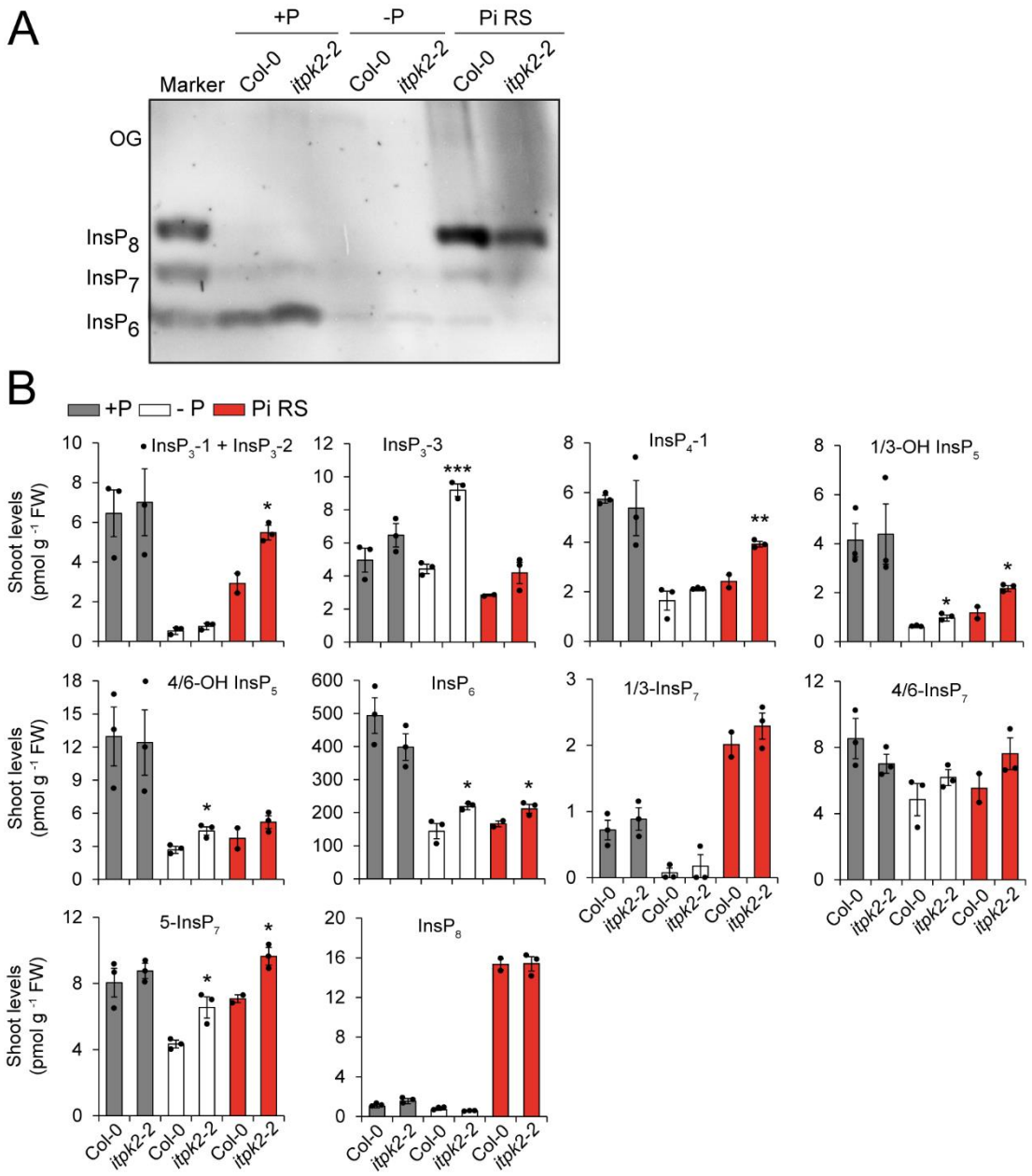

Supplemental Figure 11. P_i-dependent $InsP_7$ and $InsP_8$ synthesis is not substantially altered in shoots of the *itpk2-2* mutant.

(A and B) PAGE detection **(A)** and CE-ESI-MS analysis **(B)** of inositol (pyro)phosphates in shoots of WT and *itpk2-2* plants. Plants were grown in hydroponics under sufficient P_i (+P), after 7 days of P_i deficiency (-P) or after resupply of P_i to P_i-deficient plants for 12 h (P_i RS). Data represent means ± SE (n = 2-3 biological replicates). OG, orange G. **P* < 0.05, ***P* < 0.01 and ****P* < 0.001 denote significant difference to wild type (Col-0) according to Student's *t*-test.

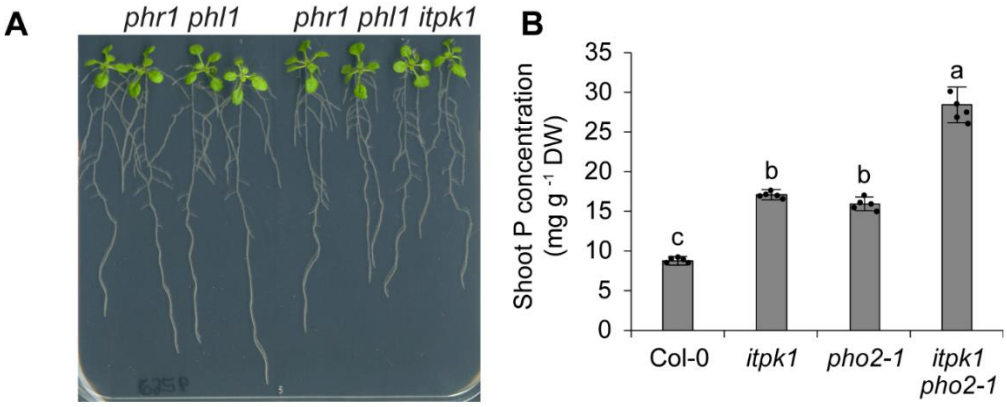

Supplemental Figure 12. The short-root phenotype of *itpk1* plants is independent of PHR1/PHL1 and evidence for the additive role of ITPK1 and PHO2 in the regulation of P_i homeostasis.

(A) Root phenotypes of *phr1 phl1* double mutant and *phr1 phl1 itpk1* triple mutant. Seven-day-old seedlings germinated on half-strength solid Murashige and Skoog agar media containing 625 μM P_i were transferred to +P (625 μM P_i) and grown for additional 7 days. Shown are representative images of the indicated mutants grown side-by-side on the same agar plate.

(B) Total P levels were assessed in shoots of 4-week-old wild-type (Col-0) and the indicated single and double mutant. Samples of above-ground tissues were collected from 5-week-old plants grown on peat-based substrate. Data represent means ± SD (n = 5 plants). Different letters indicate significant differences according to Tukey's test ($P < 0.05$).

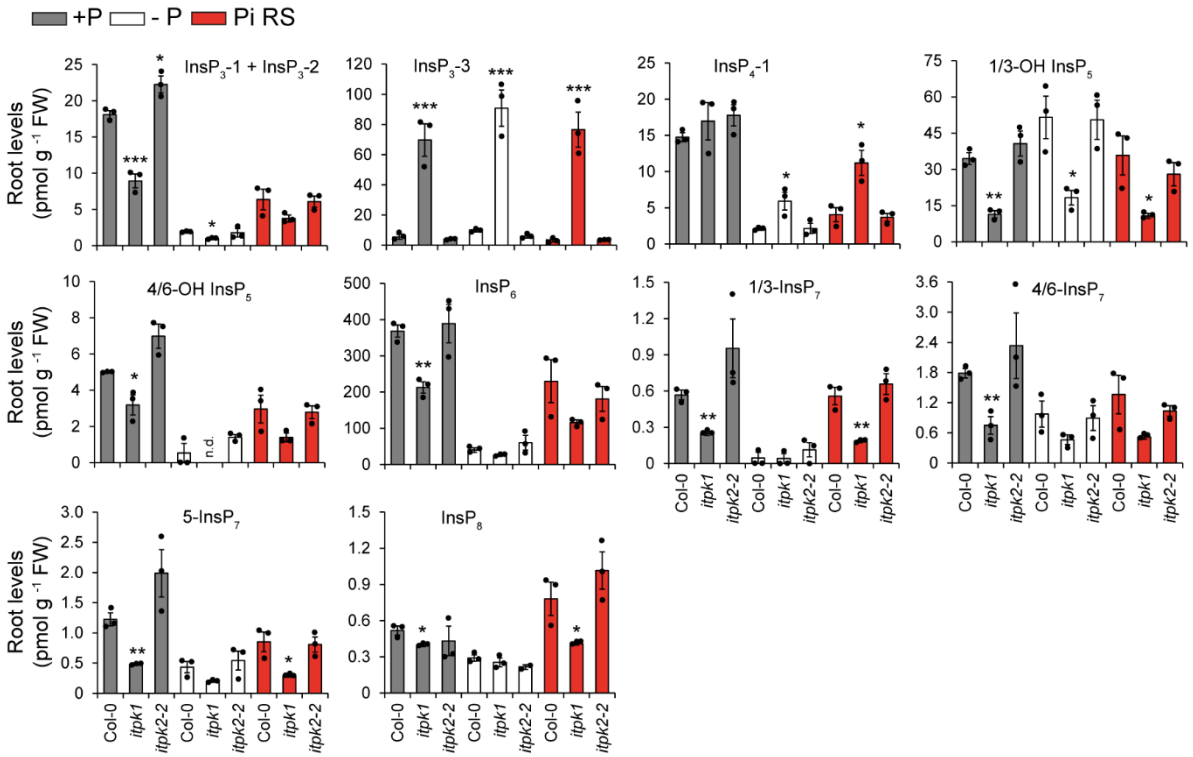

Supplemental Figure 13. ITPK1- and ITPK2-dependent inositol (pyro)phosphate metabolism in roots.
CE-ESI-MS analysis of inositol (pyro)phosphates in roots of WT (Col-0) and *itpk1* plants. Plants were cultivated in hydroponics under sufficient P_i (+P), deficient P_i for 7 days (-P) or -P resupplied with P_i for 12 h (Pi RS). Data represent means ± SE (n = 3 biological replicates). n.d., not detected. *P < 0.05, **P < 0.01 and ***P < 0.001 denote significant difference to wild type (Col-0) according to Student's t-test.

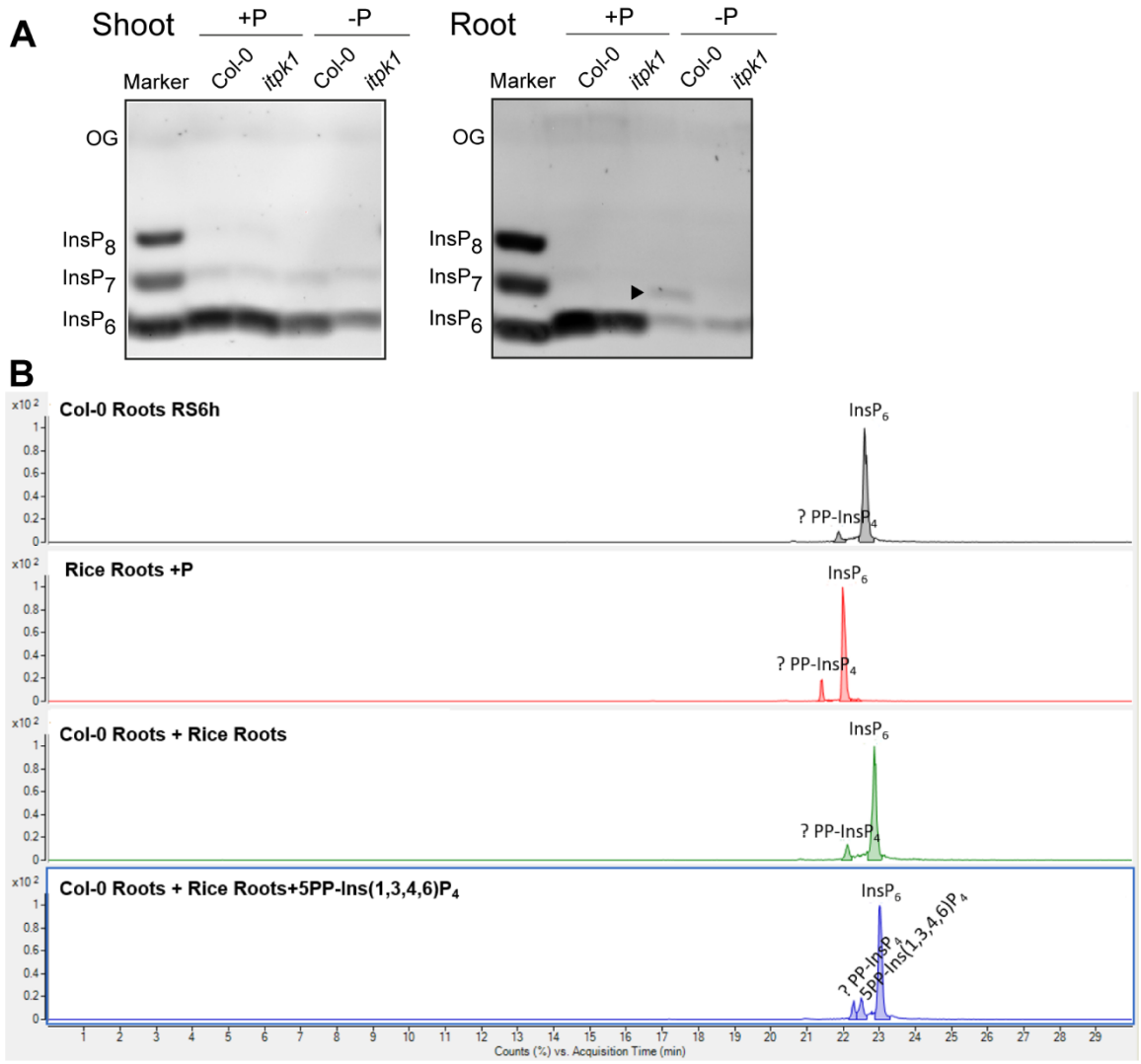

Supplemental Figure 14. Roots of *Arabidopsis* and rice plants produce a PP-InsP$_4$ isomer not previously identified in plants.

(A) PAGE detection of InsPs and PP-InsPs in shoots and roots of WT (Col-0) and *itpk1* mutant plants grown in hydroponics in P_i -sufficient solution (+P) or exposed for 7 days to P_i starvation (-P). Shown are PAGE results of shoots and roots of the same plants. The PAGE of roots is also shown in Fig. 7C and is displayed here for a direct comparison with shoot. The arrowhead indicates the appearance of a band between InsP$_6$ and InsP$_7$ specifically in WT root samples. OG, orange G.

(B) CE-ESI-MS identification of a new PP-InsP$_4$ isomer in roots of *Arabidopsis* and rice plants. The identified isomer generated in the roots of both species was indistinguishable and did not co-migrate with a 5PP-Ins(1,3,4,6)P$_4$ standard.

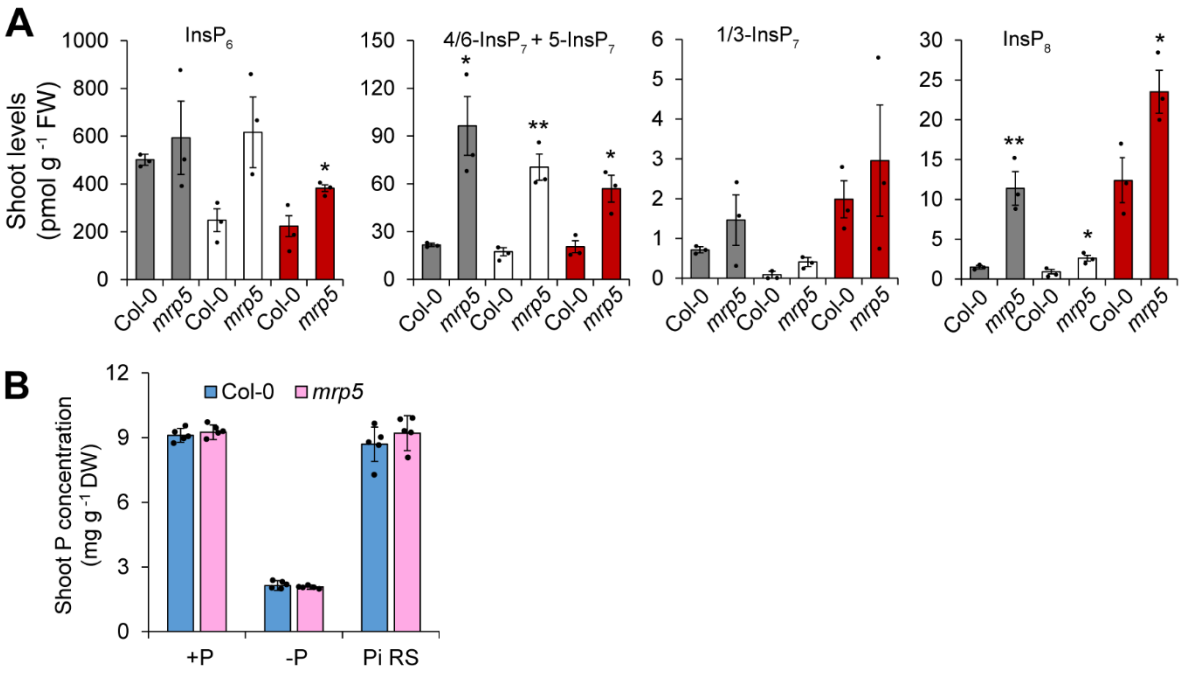

Supplemental Figure 15. Disruption of *MRP5* increases PP-InsP synthesis in shoots but does not alter P_i-dependent regulation of $InsP_8$ synthesis.

(A) CE-ESI-MS analysis of $InsP_6$ and PP-InsPs in shoots of wild-type (Col-0) and *mrp5* plants. Plants were grown in hydroponics in P_i -sufficient solution (+P), exposed for 7 days to P_i starvation (-P) or -P resupplied with P_i for 12 h (Pi RS). In this run, a baseline separation of 5-$InsP_7$ and 4/6-$InsP_7$ was not possible and combined results are shown. Data represent means ± SE (n = 3 biological replicates). **P* < 0.05 and ***P* < 0.01 denote significant difference to wild type (Col-0) according to Student's *t*-test.

(B) Total P concentration in shoots of WT (Col-0) and *mrp5* mutant plants grown as described in **(A)**. Data represent means ± SD (n = 5 plants).

Supplemental Methods

Hydroponics culture of *Arabidopsis* and rice

For hydroponic culture, *Arabidopsis* seeds were pre-cultured on rock wool moistened with tap water. After 1 week, the tap water was replaced by half-strength nutrient solution containing 2 mM NH_4NO_3, 1 mM KH_2PO_4, 1 mM $MgSO_4$, 1 mM KCl, 250 µM K_2SO_4, 250 µM $CaCl_2$, 100 µM Na-Fe-EDTA, 30 µM H_3BO_3, 5 µM $MnSO_4$, 1 µM $ZnSO_4$, 1 µM $CuSO_4$ and 0.7 µM $NaMoO_4$ (pH adjusted to 5.8 by KOH). After 7 days, the nutrient solution was changed to full-strength and replaced once a week during 2 weeks, then twice a week during 1 week, and every 2 days once the treatments were imposed. Aeration was provided to roots from the third week onwards. To induce P_i deficiency, KH_2PO_4 was replaced by KCl and P_i resupply was performed by refeeding P_i-starved plants with 1 mM KH_2PO_4 for 12 h. Plants were grown hydroponically in a growth chamber under the above-mentioned conditions except that the light intensity was 200 µmol photons m^{-2} s^{-1} and supplied by halogen lamps.

Rice plants (cv. Nipponbare) were cultivated in hydroponics inside a glasshouse with natural light supplemented with high pressure sodium vapor lamps to ensure a minimum light intensity of 300 µmol m^{-2} s^{-1}, and 30°C/25°C day (16 h)/night (8 h) temperature. Seeds were germinated in darkness at 30°C for 3 days and then transferred to meshes floating on a solution containing 0.5 mM $CaCl_2$ and 10 µM Na-Fe-EDTA, which was exchanged every third day. After 10 days, homogenous seedlings were transplanted into 60-L tanks filled with a modified Yoshida nutrient solution (Shrestha et al., 2018). Ten days later, the nutrient solution was changed to full-strength and exchanged every 10 days. During the whole growing period, the pH value was adjusted to 5.5 every second day. P_i starvation was imposed for 10 days before starting P_i resupply.

Agar plate culture of *Arabidopsis*

Cultivation of *Arabidopsis* plants under sufficient P_i (625 µM P_i) or low P_i (5 µM P_i) in sterile solid medium was performed exactly as described in Gruber et al. (2013).

Analysis of ATP and ADP

Adenosine nucleotides were specifically determined according to Haink and Deussen (2003) with some modifications. Frozen leaf material (100 mg) was homogenized in liquid N_2 and extracted with methanol/chloroform according to Ghaffari et al. (2016). An aliquot of extracted samples was used for derivatization. Twenty µL of extract was added to 205 µL of a buffer

containing 62 mM sodium citrate and 76 mM KH_2PO_4 for which pH was adjusted to 5.2 with KOH. To this mixture, 25 µL chloracetaldehyde (Sigma-Aldrich, Germany) was added and the whole solution was incubated for 40 min at 80°C followed by cooling and centrifugation for 1 min at 14000 rpm. Two blanks containing all reagents except plant extract were used as control. For quantification, external ATP and ADP standards were established with different concentrations. Separation of adenosine nucleotides was performed on a newly developed UPLC-based method using ultra pressure reversed phase chromatography (Acquity H-Class, Waters GmbH, Eschborn, Germany). The UPLC system consisted of a quaternary solvent manager, a sample manager-FTN, a column manager and a fluorescent detector (PDA eλ Detector). The separation was carried out on a C18 reversed phase column (YMC Triart, 1.9 µm, 2.0x100 mm ID, YMC Chromatography, Germany) with a flow rate of 0.6 ml per min and duration of 7 min. The column was heated at 37°C during the whole run. The detection wavelengths were 280 nm for excitation and 410 nm as emission. The gradient was accomplished with two solutions. Eluent A was 5.7 mM tetrabutylammonium bisulfate (TBAS) and 30.5 mM potassium KH_2PO_4, pH adjusted to 5.8. Eluent B was a mixture of pure acetonitrile and TBAS in a ratio of 2:1. The column was equilibrated with eluent A (90%) and eluent B (10 %) for at least 30 minutes. The gradient was produced as follow: 90% A and 10% B for 2 min, changed to 40% A and 60% B and kept for 2.3 min, changed to 10% A and 90% B for 1.1 min and reversed to 90% A and 10% B for another 1.6 min.

Supplemental References

Ghaffari, M.R., Shahinnia, F., Usadel, B., Junker, B., Schreiber, F., Sreenivasulu, N., and Hajirezaei, M.R. (2016). The metabolic signature of biomass formation in barley. Plant Cell Physiol. **57**:1943-1960.

Gruber, B.D., Giehl, R.F.H., Friedel, S., and von Wirén, N. (2013). Plasticity of the Arabidopsis root system under nutrient deficiencies. Plant Physiol. **163**:161–179.

Haink, G., and Deussen, A. (2003). Liquid chromatography method for the analysis of adenosine compounds. J. Chromatogr. B Analyt. Technol. Biomed. Life Sci. **784**:189-193.

Müller, J., Toev, T., Heisters, M., Teller, J., Moore, K.L., Hause, G., Dinesh, D.C., Burstenbinder, K., and Abel, S. (2015). Iron-dependent callose deposition adjusts root meristem maintenance to phosphate availability. Dev. Cell **33**:216-230.

Shrestha, A., Dziwornu, A.K., Ueda, Y., Wu, L.B., Mathew, B., and Frei, M. (2018). Genome-wide association study to identify candidate loci and genes for Mn toxicity tolerance in rice. Plos One 13.